1 Introduction

1.1 The origins of surveying

Since the dawn of civilization, man has looked to the heavens with awe searching for portentous signs. Some of these men became experts in deciphering the mystery of the stars and developed rules for governing life based upon their placement. The exact time to plant the crops was one of the events that was foretold by the early priest astronomers who in essence were the world's first surveyors. Today, it is known that the alignment of such structures as the pyramids and Stonehenge was accomplished by celestial observations and that the structures themselves were used to measure the time of celestial events such as the vernal equinox.

Some of the first known surveyors were Egyptian surveyors who used distant control points to replace property corners destroyed by the flooding Nile River. Later, the Greeks and Romans surveyed their settlements. The Dutch surveyor Snell van Royen was the first who measured the interior angles of a series of interconnecting triangles in combination with baselines to determine the coordinates of points long distances apart. Triangulations on a larger scale were conducted by the French surveyors Picard and Cassini to determine a baseline extending from Dunkirk to Collioure. The triangulation technique was subsequently used by surveyors as the main means of determining accurate coordinates over continental distances.

The chain of technical developments from the early astronomical surveyors to the present satellite geodesists reflects man's desire to be able to master time and space and to use science to further his society. The surveyor's role in society has remained unchanged from the earliest days; that is to determine land boundaries, provide maps of his environment, and control the construction of public works.

1.2 Development of global surveying techniques

The use of triangulation (later combined with trilateration and traversing) was limited by the line of sight. Surveyors climbed to mountain tops and developed special survey towers to extend this line of sight usually by small amounts. The series of triangles was generally oriented or fixed by astronomic points where special surveyors had observed selected stars to determine the position of that point on the surface of the earth. Since these

astronomic positions could be in error by hundreds of meters, each continent was virtually (positionally) isolated and their interrelationship was imprecisely known.

1.2.1 Optical global triangulation

Some of the first attempts to determine the interrelationship between the continents were made using the occultation of certain stars by the moon. This method was cumbersome at best and was not particularly successful. The launch of the Russian Sputnik satellite in 1957, however, had tremendously advanced the connection of the various geodetic world datums. In the beginning of the era of artificial satellites, an optical method, based (in principle) on the stellar triangulation method developed in Finland as early as 1946, was applied very successfully. The worldwide satellite triangulation program, often called the BC-4 program (after the camera that was used), for the first time determined the interrelationships of the major world datums. This method involved photographing special reflective satellites against a star background with a metric camera that was fitted with a specially manufactured chopping shutter. The image that appeared on the photograph consisted of a series of dots depicting each star's path and a series of dots depicting the satellite's path. The coordinates of selected dots were precisely measured using a photogrammetric comparator, and the associated spatial directions from the observing site to the satellite were then processed using an analytical photogrammetric model. Photographing the same satellite from a neighboring site simultaneously and processing the data in an analogous way yields another set of spatial directions. Each pair of corresponding directions forms a plane containing the observing points and the satellite, and the intersection of at least two planes results in the spatial direction between the observing sites. In the next step, these oriented directions were used to construct a global network with the scale being derived from several terrestrial traverses. An example is the European baseline running from Tromsø in Norway to Catania on Sicily. The main problem in using this optical technique was that clear sky was required simultaneously at a minimum of two observing sites separated by some 4 000 km, and the equipment was massive and expensive. Thus, optical direction measurement was soon supplanted by the electromagnetic ranging technique because of all-weather capability, greater accuracy, and lower cost of the newer technique.

1.2.2 Electromagnetic global trilateration

First attempts to (positionally) connect the continents by electromagnetic techniques was by the use of an electronic ranging system (HIRAN) developed during World War II to position aircraft. Beginning in the late 1940s, HIRAN arcs of trilateration were measured between North America and Europe in an attempt to determine the difference in their respective datums. A significant technological breakthrough occurred in 1957 after the launch of Sputnik, the first artificial satellite, when scientists around the world experienced that the Doppler shift in the signal broadcast by a satellite could be used as an observable to determine the exact time of closest approach of the satellite. This knowledge, together with the ability to compute satellite ephemerides according to Kepler's laws, led to the present capability of instantaneously determining precise position anywhere in the world.

The immediate predecessor of today's modern positioning system is the Navy Navigation Satellite System (NNSS), also called TRANSIT system. This system was composed of six satellites orbiting at altitudes of about 1 100 km with nearly circular polar orbits. The TRANSIT system was developed by the U.S. military, primarily, to determine the coordinates of vessels and aircraft. Civilian use of this satellite system was eventually authorized, and the system became widely used worldwide both for navigation and surveying.

Some of the early TRANSIT experiments by the former U.S. Defense Mapping Agency (DMA) and the U.S. Coast & Geodetic Survey showed that accuracies of about one meter could be obtained by occupying a point for several days and reducing the observations using the postprocessed precise ephemerides. Groups of Doppler receivers in translocation mode could also be used to determine the relative coordinates of points to submeter accuracy using the broadcast ephemerides. This system employed essentially the same Doppler observable used to track the Sputnik satellite; however, the orbits of the TRANSIT satellites were precisely determined by tracking them at widely spaced fixed sites.

1.3 History of the Global Positioning System

The Global Positioning System (GPS) was developed to replace the TRANSIT system because of two major shortcomings in the earlier system. The large time gaps in coverage were the main problem with TRANSIT. Since nominally a satellite passed overhead every 90 minutes, users had to interpolate their position between "fixes" or passes. The second problem with the TRANSIT system was its relatively low navigation accuracy.

In contrast, GPS answers the questions "What time, what position, and what velocity is it?" quickly, accurately, and inexpensively anywhere on the globe at any time.

1.3.1 Navigating with GPS

One aim of navigation is instantaneous positioning and velocity determination. As stated, one of the main problems with the TRANSIT system was the fact that it was not able to provide continuous positioning.

Satellite constellation
To provide a continuous global positioning capability, a scheme to orbit a sufficient number of satellites to ensure that (at least) four were always electronically visible was developed for GPS. Several schemes were proposed and it was found that 24 evenly spaced satellites placed in circular 12-hour orbits inclined 55° to the equatorial plane would provide the desired coverage for the least expense. In any event, this constellation provides the minimum of four satellites in good geometric position 24 hours per day anywhere on the earth. There are often more than the minimum number of satellites available for use and it is during these periods that surveyors perform special surveys. In fact, assuming a 10° elevation angle, there are brief periods where up to 10 GPS satellites are visible on the earth.

Point positioning
The GPS satellites are configured, primarily, to provide the user with the capability of determining his position, expressed for example by latitude, longitude, and elevation. This is accomplished by the simple resection process using the distances measured to satellites.

Consider the satellites frozen in space at a given instant. The space coordinates $\underline{\varrho}^S$ relative to the center of the earth of each satellite (see also Fig. 1.1) can be computed from the ephemerides broadcast by the satellite by an algorithm presented in Chap. 4. If the ground receiver defined by its geocentric position vector $\underline{\varrho}_R$ employed a clock that was set precisely to GPS system time (Sect. 3.3) the true distance or range ϱ to each satellite could be accurately measured by recording the time required for the (coded) satellite signal to reach the receiver. Each range defines a sphere (more precisely: surface of a sphere) with its center at the satellite. Hence, using this technique, ranges to only three satellites would be needed since the intersection of three spheres yields the three unknowns (e.g., latitude, longitude, and height) which could be determined from the three range equations

$$\varrho = \|\underline{\varrho}^S - \underline{\varrho}_R\| \,. \tag{1.1}$$

GPS receivers apply a slightly different technique. They typically use an inexpensive crystal clock which is set approximately to GPS time. Thus, the clock of the ground receiver is offset from true GPS time, and because

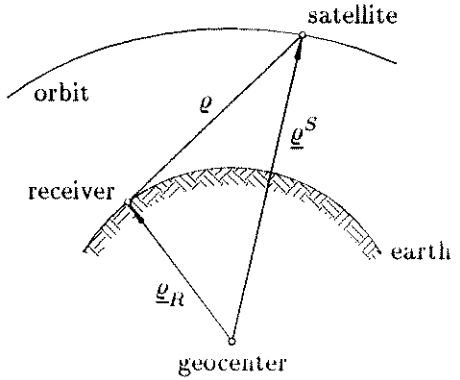

Fig. 1.1. Principle of satellite positioning

of this offset, the distance measured to the satellite differs from the "true" range. These distances are called pseudoranges R since they are the true range plus a range correction $\Delta\varrho$ resulting from the receiver clock error or bias δ. A simple model for the pseudorange is

$$R = \varrho + \Delta\varrho = \varrho + c\,\delta \tag{1.2}$$

with c being the velocity of light.

Four simultaneously measured pseudoranges are needed to solve for the four unknowns; these are three components of position plus the clock bias. Geometrically, the solution is accomplished by a sphere being tangent to the four spheres defined by the pseudoranges. The center of this sphere corresponds to the unknown position and its radius equals the range correction.

It is worth noting that the range error $\Delta\varrho$ could be eliminated in advance by differencing the pseudoranges measured from one site to two satellites or two different positions of one satellite. In the second case, the resulting range difference or delta range corresponds to the observable in the TRANSIT system. In both cases, the delta range defines a hyperboloid with its foci placed at the two satellites or the two different satellite positions for the geometric location of the receiver.

Considering the fundamental equation (1.1), one can conclude that the accuracy of the position determined using a single receiver essentially is affected by the following factors:

- accuracy of each satellite position,
- accuracy of pseudorange measurement,
- geometry.

Systematic errors in the satellite position and eventual satellite clock biases in the pseudoranges can be reduced or eliminated by differencing the pseudoranges measured from two sites to the satellite. This interferometric approach has become fundamental for GPS surveying as demonstrated below. However, no mode of differencing can overcome poor geometry.

A measure of satellite geometry with respect to the observing site is a factor known as Geometric Dilution of Precision (GDOP). In a geometric approach, this factor is inversely proportional to the volume of a body. This body is formed by points obtained from the intersection of a unit sphere with the vectors pointing from the observing site to the satellites. More details and an analytical approach on this subject are provided in Sect. 9.6.

Velocity determination
The determination of the instantaneous velocity of a moving vehicle is another goal of navigation. This can be achieved by using the Doppler principle of radio signals. Because of the relative motion of the GPS satellites with respect to a moving vehicle, the frequency of a signal broadcast by the satellites is shifted when received at the vehicle. This measurable Doppler shift is proportional to the relative radial velocity. Since the radial velocity of the satellites is known, the radial velocity of the moving vehicle can be deduced from the Doppler observable. A minimum of four Doppler observables is required to solve for the three components of the vehicle's velocity vector and, possibly, one frequency bias.

In summary, GPS was designed to solve many of the problems inherent to the TRANSIT system. Above all, GPS provides 24 hours a day instantaneous global navigation. The system as originally designed, however, did not include provision for the accurate surveying that is performed today. This surveying use of GPS resulted from a number of fortuitous developments described below.

1.3.2 Surveying with GPS

From navigation to surveying
As previously described, the use of near-earth satellites for navigation was demonstrated by the TRANSIT system. In 1964, I. Smith filed a patent describing a satellite system that would emit time codes and radio waves that would be received on earth as time delayed transmissions creating hyperbolic lines of position. This concept would become important in the treatment of GPS observables to compute precise vectors. A few years later, another patent was filed by R. Easton further refining the concept of comparing the

phase from two or more satellites.

In 1972, C. Counselman along with colleagues from the Massachusetts Institute of Technology (MIT) reported on the first use of interferometry to track the Apollo 16 Lunar Rover module. The principle they described is in essence the same technique they used later in developing the first geodetic GPS receiver and corresponds to differencing pseudoranges measured from two receivers to one satellite. The present use of the GPS carrier phase to make millimeter vector measurements dates from work by the MIT group using Very Long Baseline Interferometry (VLBI) performed between 1976 and 1978 where they proved that (for short lines) millimeter accuracy was obtainable using the interferometric technique.

In 1978, the Miniature Interferometer Terminals for Earth Surveying (MITES) were proposed. They detail how a satellite system can be used for precise surveying. This concept was further refined to include the Navigation System with Timing and Ranging (NAVSTAR). Also, the codeless technique that later became important in developing high-accuracy dual frequency receivers was described for the first time.

Observation techniques
When referring to high accuracy, GPS surveying implies the precise measurement of the vector between two (or more) GPS receivers.

The observation technique where both receivers involved remain fixed in position is called static surveying. The static method formerly required hours of observation and was the technique that was primarily used for early GPS surveys. A second technique where one receiver remains fixed, while the second receiver moves is called kinematic surveying. In 1986, B. Remondi first demonstrated that subcentimeter vector accuracies could be obtained between a pair of GPS survey instruments with as little as a few seconds of data collection using this method. B. Remondi also first developed another survey technique which is denoted as pseudokinematic technique. In this technique, a pair of receivers occupies a pair of points for two brief periods that are separated in time. This method, also denoted intermittent static, snapshot static, or reoccupation has demonstrated accuracies comparable to the static method.

Data processing is performed in two conceptually different ways. (1) Relative positioning is the technique where simultaneously observed data are processed; strictly speaking, the result is not obtainable instantaneously due to the required simultaneity. (2) The differential positioning technique involves placing one receiver at a fixed site of known position. Comparing computed ranges with measured pseudoranges, the reference site can transmit corrections to a roving receiver to improve its measured pseudoranges.

This technique provides instantaneous positioning and is, thus, mainly applied in kinematic surveys.

Hardware developments
The following sections contain reference to various terms that are more fully described in subsequent chapters. These are the C/A-code (Coarse/Acquisition) and P-code (Precision) which are basically code bits that are modulated on the two carrier signals broadcast by the GPS satellites. Code correlation as well as codeless techniques strip these codes from the carrier so that the phase of the (reconstructed) carrier can be measured. Brand names mentioned in this section are included for historical purposes since they represent the first of a certain class or type of receiver.

An interferometric technology for codeless pseudoranging was developed by P. MacDoran at the Jet Propulsion Laboratory (JPL). This Satellite Emission Range Inferred Earth Surveying (SERIES) technique was later improved for commercial geodetic applications. The culmination of the VLBI interferometric research applied to earth orbiting satellites was the production of a "portable" codeless GPS receiver that could measure short baselines to millimeter accuracy and long baselines to one part per million (ppm). This performance of the receiver, trade-named the Macrometer Interferometric Surveyor™, was demonstrated by the former U.S. Federal Geodetic Control Committee (FGCC).

A parallel development was being carried out by the DMA in cooperation with the U.S. National Geodetic Survey (NGS) and the U.S. Geological Survey (USGS). In 1981, these agencies developed specifications for a portable dual frequency code correlating receiver that could be used for precise surveying and point positioning. Texas Instruments Company was awarded the contract to produce a receiver later trade-named the TI-4100. The NGS geodesists C. Goad and B. Remondi developed software to process its carrier phase data in a manner similar to the method used by the MIT group (i.e., interferometrically).

The physical characteristics of the TI-4100 were significantly different from the Macrometer. The TI-4100 was a dual frequency receiver that used the P-code to track a maximum of four satellites, while the original Macrometer was a rack mounted codeless single frequency receiver that simultaneously tracked up to six satellites. There were also significant logistic differences in performing surveys using these two pioneer instruments. The TI-4100 received the broadcast ephemerides and timing signals from the GPS satellites so units could be operated independently, while the Macrometer required that all units be brought together prior to the survey and after the survey so that the time of the units could be synchronized. Also, the Macrometer

required that the ephemerides for each day's tracking be generated at the home office prior to each day's observing session.

The next major development in GPS surveying occurred in 1985 when manufacturers started to produce C/A-code receivers that measured and output the carrier phase. The first of this class of receivers was trade-named the Trimble 4000S. This receiver required the data to be collected on an external (i.e., laptop) computer. The 4000S was the first of the generic C/A-code receivers that eventually were produced by a host of manufacturers. The first Trimble receivers were sold without processing software; however, the company soon retained the services of C. Goad who produced appropriate vector computation software which set the standard for future software developers.

Today's GPS receivers include all features of the early models and additionally have expanded capabilities. By far the major portion of receivers produced today are the C/A-code single frequency type. For precise geodetic work, however, the more expensive dual frequency receivers are the standard.

Software developments
The development of GPS surveying software has largely paralleled the development of hardware.

The NGS has been one of the primary organizations in the world in developing independent GPS processing software. As previously mentioned, C. Goad and B. Remondi pioneered this development.

The NGS first produced processing software that used the Macrometer phase measurements and the precise ephemerides produced by the U.S. Naval Surface Warfare Center (NSWC). Other Macrometer users had to apply the processing software developed by the Macrometer manufacturer which required the use of specially formatted ephemerides produced (and sold) by them. The NGS software was also adapted for the TI-4100 format data and finally for other receivers that were subsequently used.

The original software developed by both the NGS and manufacturers computed individual vectors one at a time. These vectors were then combined in a network or geometric figure, and the coordinates of all points were determined using least squares adjustment programs.

The NGS and the Macrometer manufacturer eventually developed processing software that simultaneously determined all vectors observed during a given period of time (often called session). The second generation multibaseline software included the ability to determine corrections to the satellite orbits and was often called orbital relaxation software. This technique was pioneered by G. Beutler's group at the Bernese Astronomical Institute. To-

day, relaxation software is no longer applied since precise orbital information is available to the public.

Today, a huge number of scientific as well as commercial software is available. A review of software features is given in Chap. 11.

Ephemerides service
The first GPS surveys performed in late 1982 using Macrometers depended on orbital data derived from a private tracking network. Later, the broadcast ephemerides were used to supplement this private tracking data. The TI-4100 receiver obtained the ephemerides broadcast by the satellites so that processing programs could use this ephemerides to process vectors. The NSWC originally processed the military ephemerides obtaining "precise" postprocessed ephemerides which were turned over to the NGS for limited distribution to the public.

Today, various organizations around the world provide satellite tracking data from points that are referenced to a global datum. The tracking stations collect code range and phase data for both frequencies for all satellites. The data are processed and archived on a daily basis. Precise ephemerides are now available within a few days to the public upon request.

2 Overview of GPS

2.1 Basic concept

The Global Positioning System is the responsibility of the Joint Program Office (JPO), a component of the Space and Missile Center at El Segundo, California. In 1973, the JPO was directed by the U.S. Department of Defense (DoD) to establish, develop, test, acquire, and deploy a spaceborne positioning system. The present Navigation System with Timing and Ranging (NAVSTAR) Global Positioning System (GPS) is the result of this initial directive.

The Global Positioning System was conceived as a ranging system from known positions of satellites in space to unknown positions on land, at sea, in air and space. Effectively, the satellite signal is continually marked with its (own) transmission time so that when received the signal transit period can be measured with a synchronized receiver. The original objectives of GPS were the instantaneous determination of position and velocity (i.e., navigation), and the precise coordination of time (i.e., time transfer). A detailed definition given by W. Wooden in 1985 reads:

"The Navstar Global Positioning System (GPS) is an all-weather, space-based navigation system under development by the Department of Defense (DoD) to satisfy the requirements for the military forces to accurately determine their position, velocity, and time in a common reference system, anywhere on or near the Earth on a continuous basis."

Since the DoD is the initiator of GPS, the primary goals were military ones. But the U.S. Congress, with guidance from the President, directed DoD to promote its civil use. This was greatly accelerated by employing the Macrometer for geodetic surveying. This instrument was in commercial use at the time the military was still testing navigation receivers so that the first productive application of GPS was to establish high-accuracy geodetic networks.

As previously stated, GPS uses pseudoranges derived from the broadcast satellite signal. The pseudorange is derived either from measuring the travel time of the (coded) signal and multiplying it by its velocity or by measuring the phase of the signal. In both cases, the clocks of the receiver and the satellite are employed. Since these clocks are never perfectly synchronized, instead of true ranges "pseudoranges" are obtained where the synchronization error (denoted as clock error) is taken into account, cf. Eq. (1.2). Consequently, each equation of this type comprises four unknowns: the three

November 26, 1990. Today, no distinction is made between Block II and Block IIA satellites.

The Block IIR satellites ("R" denotes replenishment or replacement) weigh more than 2 000 kg and the $42 million cost are about the same as for the Block II's. The first Block IIR satellite was successfully launched on July 23, 1997 and 19 more launches are expected to follow. These satellites have a design life of 10 years. They are equipped with improved facilities for communication and intersatellite tracking. Satellites launched after 2005 will also transmit additional signal components.

The Block IIF satellites ("F" denotes follow on) will weigh more than 2 000 kg and will be launched from 2007 onwards. These satellites will have a design life of 15 years. They will be equipped with improved on-board capabilities (such as inertial navigation systems) and an augmented signal structure. An artist's rendering of a Block IIF satellite is shown on the front cover of this textbook.

Presently, the DoD undertakes studies for the next generation of GPS satellites, called Block III satellites. These satellites are expected to carry GPS into 2030 and beyond.

Satellite signal

The actual carrier broadcast by the satellite is a spread spectrum signal that makes it less subject to intentional (or unintentional) jamming. The spread spectrum technique is commonly used today by such diverse equipment as hydrographic positioning ranging systems and wireless local area network systems.

The key to the system's accuracy is the fact that all signal components are precisely controlled by atomic clocks. The Block II satellites have four on-board time standards, two rubidium and two cesium clocks. The long-term frequency stability of these clocks reaches a few parts in 10^{-13} and 10^{-14} over one day. The future hydrogen masers will have an even better stability of 10^{-14} to 10^{-15} over one day. These highly accurate frequency standards being the heart of GPS satellites produce the fundamental L-band frequency of 10.23 MHz. Coherently derived from this fundamental frequency are (presently) two signals, the L1 and the L2 carrier waves generated by multiplying the fundamental frequency by 154 and 120 respectively yielding

$$L1 = 1575.42 \text{ MHz},$$
$$L2 = 1227.60 \text{ MHz}.$$

These dual frequencies are essential for eliminating the major source of error, i.e., the ionospheric refraction (Sect. 6.3.2).

The pseudoranges that are derived from measured travel times of the signal from each satellite to the receiver use two pseudorandom noise (PRN) codes that are modulated (superimposed) onto the two base carriers.

The first code is the C/A-code (Coarse/Acquisition-code) which is available for civilian use. The C/A-code, designated as the Standard Positioning Service (SPS), has an effective wavelength of approximately 300 m. The C/A-code is presently modulated upon L1 only and is purposely omitted from L2. This omission allows the JPO to control the information broadcast by the satellite and, thus, denies full system accuracy to nonmilitary users.

The second code is the P-code (Precision-code) which has been reserved for U.S. military and other authorized users. The P-code, designated as the Precise Positioning Service (PPS), has an effective wavelength of approximately 30 m. The P-code is modulated on both carriers L1 and L2. Unlimited access to the P-code was permitted until the system was declared fully operational.

In addition to the PRN codes, a data message is modulated onto the carriers consisting of status information, satellite clock bias, and satellite ephemerides. A detailed signal description is given in Sect. 5.1.

It is worth noting that the present signal structure will be improved in the near future (Sect. 13.2).

2.2.3 Operational capabilities

There are two operational capabilities: (1) Initial Operational Capability (IOC) and (2) Full Operational Capability (FOC).

IOC was attained in July 1993 when 24 (Block I/II/IIA) GPS satellites were operating and were available for navigation. Officially, IOC was declared by the DoD on December 8, 1993.

FOC was achieved when 24 Block II/IIA satellites were operational in their assigned orbits and the constellation was tested for operational military performance. Even though 24 Block II and Block IIA satellites were available since March 1994, FOC was not declared before July 17, 1995.

2.2.4 Denial of accuracy and access

Two techniques are known for denying civilian users full use of the system. The first is Selective Availability (SA) and the second is Anti-spoofing (A-S).

Selective availability

Originally, the accuracy expected from C/A-code pseudorange positioning was in the range of some 400 m. Field tests achieved the surprising level of navigation accuracy of 15–40 m for positioning and a fraction of a meter

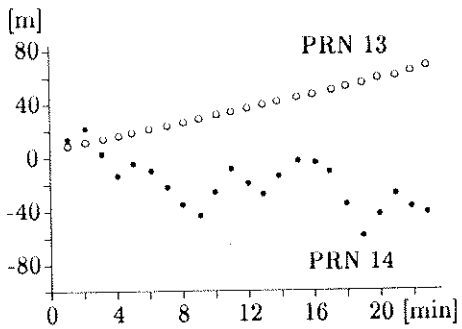

Fig. 2.1. Satellite clock behavior of PRN 13 (without SA) and of PRN 14 (with SA) on day 177 of 1992 after Breuer et al. (1993)

per second for velocity. The goal of SA was to deny this navigation accuracy to potential adversaries by dithering the satellite clock (δ-process) and manipulating the ephemerides (ε-process).

The δ-process is achieved by dithering the fundamental frequency of the satellite clock. The satellite clock bias has a direct impact on the pseudorange which is derived from a comparison of the satellite clock and the receiver clock. Since the fundamental frequency is dithered, code and carrier pseudoranges are affected in the same way. In Fig. 2.1, the different behavior of satellite clocks with and without SA is shown. With SA activated, there are variations of the pseudoranges with amplitudes of some 50 m and with periods of some minutes. When pseudoranges are differenced between two receivers, the dithering effect is eliminated.

The ε-process is the truncation of the orbital information in the transmitted navigation message so that the coordinates of the satellites cannot accurately be computed. The error in satellite position roughly translates to a like position error of stand-alone receivers. For baselines, the relative satellite position errors are (approximately) equal to the relative baseline errors. In Fig. 2.2, the behavior of the radial orbit error with and without SA is shown. In the case of SA, there are variations with amplitudes between 50 m and 150 m and with periods of some hours. The orbital errors cause pseudorange errors with similar characteristics. Thus, these errors are highly reduced when pseudoranges are differenced between two receivers,

SA has been in force since March 25, 1990. According to the specifications of the DoD, the accuracy for stand-alone receivers was degraded to 100 m for horizontal position and to 156 m for height. These specifications also implied a velocity error of 0.3 m s^{-1} and an error in time of 340 ns. All numbers are given at the 95% probability level. At the 99.99% probability

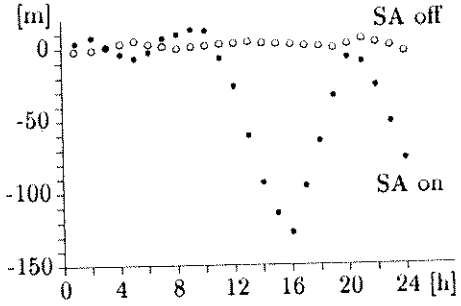

Fig. 2.2. Radial orbit error of PRN 21 on day 177 of 1992 with SA on and on day 184 of 1992 with SA off after Breuer et al. (1993)

level, the predictable accuracy decreased to 300 m for horizontal position and to 500 m for height (Department of Defense 1995).

Due to the undermined military effectiveness of SA by applying differential techniques, a joint recommendation of the U.S. National Academy of Public Administration and a committee of the National Research Council has proposed that SA should immediately be turned to zero and deactivated after some years (CGSIC 1995). The official answer to this proposal was released on March 29, 1996 in form of the Presidential Decision Directive (PDD) on GPS. The PDD expressed the intention to discontinue the use of SA within a decade in a manner that allows adequate time and resources for the military forces to prepare fully for operations without SA. In addition, the permanent Interagency GPS Executive Board (IGEB) was established. This board is commonly chaired by the DoD and the Department of Transportation (DoT) to balance military and civil interests. The full text of the public release statement on the PDD is published, e.g., in *GPS World* 1996, 7(5), page 50.

Somehow surprisingly, SA was turned off on May 2, 2000 at about 4:00 Universal Time (UT) after an announcement of the White House one day before. The benefits for civilian users are discussed in a fact sheet released by the U.S. Department of Commerce (2000). A prediction of the world after SA is given in Conley and Lavrakas (1999) and first experiences with SA off are discussed in Conley (2000), Jong (2000). One impressive result is presented in Fig. 2.3. Although the accuracy for stand-alone receivers is improved by a factor of ten, it must be kept in mind that despite turning off SA military advantages are ensured by new developments. One of these developments is Selective Denial (SD) which will deny access to the GPS signal for unauthorized users in regions of interest by ground-based jammers

point coordinates contained in the true range, and the clock error. Thus, four satellites are necessary to solve for the four unknowns. Indeed, the GPS concept assumes that four or more satellites are in view at any location on earth 24 hours a day. The solution becomes more complicated when using the measured phase. This observable is ambiguous by an integer number of signal wavelengths so that the model for phase pseudoranges is augmented by an initial bias, also called integer ambiguity.

The all-weather global system managed by the JPO consists of three segments:

- the space segment consisting of satellites which broadcast signals,
- the control segment steering the whole system,
- the user segment including the many types of receivers.

2.2 Space segment

2.2.1 Constellation

The GPS satellites have nearly circular orbits with an altitude of about 20 200 km above the earth and a period of approximately 12 sidereal hours. The constellation and the number of satellites used have evolved from earlier plans for a 24-satellite and 3-orbital plane constellation, inclined 63° to the equator. Later, for budgetary reasons, the space segment was reduced to 18 satellites, with three satellites in each of six orbital planes. This scheme was eventually rejected, since it did not provide the desired 24-hour worldwide coverage. In about 1986, the number of satellites planned was increased to 21, again three each in six orbital planes, and three additional active spares. The spare satellites were designated to replace malfunctioning "active" satellites. The present nominal constellation consists of 24 operational satellites deployed in six evenly spaced planes (A to F) with an inclination of 55° and with four satellites per plane. Furthermore, up to four active spare satellites for replenishment will be operational (Graviss 1992).

With the full constellation, the space segment provides global coverage with four to eight simultaneously observable satellites above 15° elevation at any time of day. If the elevation mask is reduced to 10°, occasionally up to 10 satellites will be visible; and if the elevation mask is further reduced to 5°, occasionally 12 satellites will be visible.

2.2.2 Satellites

General remarks

The GPS satellites, essentially, provide a platform for radio transceivers, atomic clocks, computers, and various ancillary equipment used to operate

the system. The electronic equipment of each satellite allows the user to measure a pseudorange R to the satellite, and each satellite broadcasts a message which allows the user to determine the spatial position $\underline{\varrho}^S$ of the satellite for arbitrary instants. Given these capabilities, users are able to determine their position $\underline{\varrho}_R$ on or above the earth by resection (Fig. 1.1). The auxiliary equipment of each satellite, among others, consists of solar panels for power supply and a propulsion system for orbit adjustments and stability control.

The satellites have various systems of identification: launch sequence number, assigned pseudorandom noise (PRN) code, orbital position number, NASA catalogue number, and international designation. In agreement with the satellite navigation message and to avoid any confusion, the PRN number will be used throughout this textbook.

Satellite categories

There are six classes or types of GPS satellites. These are the Block I, Block II, Block IIA, Block IIR, Block IIF, and Block III satellites. Detailed information on launch dates, orbital position (designation letter for orbital plane plus number) and operational periods can be found on the Web site of the U.S. Coast Guard Navigation Center under http://www.navcen.uscg.mil/gps/geninfo/constell.htm.

Eleven Block I satellites (weighing 845 kg) were launched in the period between 1978 to 1985 from Vandenberg AFB, California, with Atlas F launch vehicles. With the exception of one booster failure in 1981, all launches were successful. Today, none of the original Block I satellites is in operation. Considering the 4.5-year design life of these satellites, however, it is remarkable that some of the Block I satellites were operational for more than 10 years.

The Block II constellation is slightly different from the Block I constellation since the inclination of their orbital planes is 55° compared to the former 63° inclination. Apart from orbital inclination, there is an essential difference between Block I and Block II satellites related to U.S. national security. Block I satellite signals were fully available to civilian users, while some Block II satellite signals are restricted.

The first Block II satellite, costing approximately $ 50 million and weighing more than 1 500 kg, was launched on February 14, 1989 from the Kennedy Space Center, Cape Canaveral AFB in Florida, using a Delta II Rocket. The design life of the Block II satellites is 7.5 years. Individual satellites, however, remained operational more than 10 years.

The Block IIA satellites ("A" denotes advanced) are equipped with mutual communication capability. Some of them carry retroreflectors and can be tracked by Laser ranging. The first Block IIA satellite was launched on

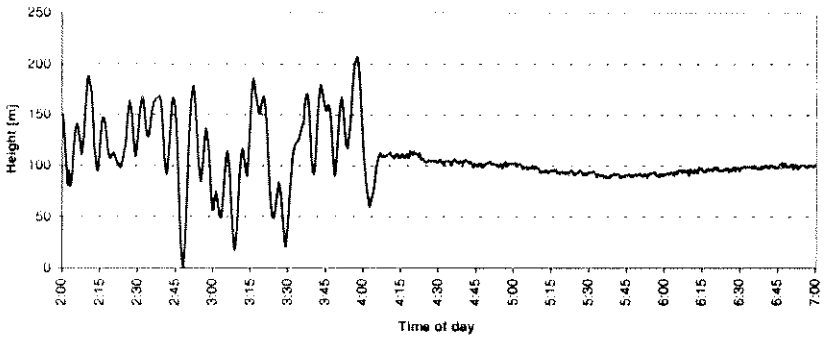

Fig. 2.3. Height variation in the station Kootwijk (The Netherlands) during the SA transition on May 2, 2000 (courtesy K. de Jong, Delft)

Anti-spoofing
The design of GPS includes the ability to essentially "turn off" the P-code or invoke an encrypted code as a means of denying access to the P-code to all but authorized users. The rationale for doing this is to keep adversaries from sending out false signals with the GPS signature to create confusion and cause users to misposition themselves.

A-S is accomplished by the modulo 2 sum of the P-code and an encrypting W-code. The resulting code is denoted as the Y-code. Thus, when A-S is active, the P-code on the L1 and the L2 carrier is replaced by the unknown Y-code. Note that A-S is either on or off. A variable influence of A-S (as was the case with SA) cannot occur.

For testing purposes, A-S was first turned on over the weekend of August 1, 1992 and later for several periods. It was expected that A-S would be switched on permanently when FOC had been attained; however, A-S was permanently implemented on January 31, 1994. In accordance with the DoD policy, no advance announcement of the implementation date was made.

The future signal structure will provide the C/A-code on both the L1 and the L2 carrier. Instead of the Y-code, a new military split-spectrum signal, denoted as M-code, will be introduced. This feature will make A-S superfluous.

2.3 Control segment

The Operational Control System (OCS) consists of a master control station, monitor stations, and ground control stations. The main operational tasks of the OCS are: tracking of the satellites for the orbit and clock determination and prediction, time synchronization of the satellites, and upload of the data

message to the satellites. The OCS was also responsible for imposing SA on the broadcast signals. The OCS performs many nonoperational activities, such as procurement and launch activities, that will not be addressed here.

Note that the control segment will be improved within the next ten years during the GPS modernization process.

2.3.1 Master control station

The location of the master control station was first at Vandenberg AFB, California, but has been moved to the Consolidated Space Operations Center (CSOC) at Shriver AFB (formerly known as Falcon AFB), Colorado Springs, Colorado. CSOC collects the tracking data from the monitor stations and calculates the satellite orbit and clock parameters using a Kalman estimator. These results are then passed to one of the three ground control stations for eventual upload to the satellites. The satellite control and system operation is also the responsibility of the master control station.

2.3.2 Monitor stations

There are five monitor stations located at: Hawaii, Colorado Springs, Ascension Island in the South Atlantic Ocean, Diego Garcia in the Indian Ocean, and Kwajalein in the North Pacific Ocean. Each of these stations is equipped with a precise atomic time standard and receivers which continuously measure pseudoranges to all satellites in view. Pseudoranges are measured every 1.5 seconds and, using the ionospheric and meteorological data, they are smoothed to produce 15-minute interval data which are transmitted to the master control station.

The tracking network described above is the official network for determining the broadcast ephemerides as well as modeling the satellite clocks. The data of up to 14 additional sites operated by the National Imagery and Mapping Agency (NIMA) are used to compute the precise ephemerides. Other tracking networks exist. These networks generally have no part in managing the system. A private tracking network was operated by the manufacturer of the Macrometer during the early 1980s. Today, more globally oriented tracking networks are operated. More details on this subject are provided in Sect. 4.4.1.

2.3.3 Ground control stations

These stations collocated with the monitor stations at Ascension, Diego Garcia, and Kwajalein are the communication links to the satellites and mainly consist of the ground antennas. The satellite ephemerides and clock

information, calculated at the master control station and received via communication links, are uploaded to each GPS satellite via S-band radio links. Formerly, uploading to each satellite was performed every eight hours; then the rate has been reduced to once (or twice) per day (Remondi 1991b). If a ground station becomes disabled, prestored navigation messages are available in each satellite to support a prediction span so that the positioning accuracy degrades quite gradually. The durations of positioning service of the satellites without contact from the OCS are given in Table 2.1.

Table 2.1. Positioning service without contact from the control segment

Block	Duration
I	3–4 days
II	14 days
IIA	180 days
IIR	>180 days

2.4 User segment

2.4.1 User categories

Military user
Strictly speaking, the term "user segment" is related to the DoD concept of GPS as an adjunct to the national defense program. Even during the early days of the system, it was planned to incorporate a GPS receiver into virtually every major defense system. It was envisioned that every aircraft, ship, land vehicle, and even groups of infantry would have an appropriate GPS receiver to coordinate their military activities. In fact, many GPS receivers were used as planned during, e.g., the 1991 Gulf War under combat conditions. In this war, SA which had been previously invoked was turned off so that troops could use more readily available civilian receivers. Handheld C/A-code receivers were particularly useful in navigating the desert.

There are various other military uses that have been proposed. One example is a receiver that can be connected to four antennas. When the antennas are placed in a fixed array (e.g., corners of a square), the attitude of the array can be determined in addition to its position. For example, placing antennas on the bow, stern, and port and starboard points of a ship would result in the determination of pitch, roll, yaw, and position of the vessel.

Civilian user
The civilian use of GPS occurred several years ahead of schedule in a manner not envisioned by the system's planners. The primary focus in the first few years of the system's development was on navigation receivers. As previously described in Chap. 1, the SERIES technique at JPL and the development of the Macrometer by C. Counselman started the GPS surveying revolution. The primary concept of using an interferometric rather than Doppler solution model meant that GPS could be used for not only long line geodetic measurements but also for the most exacting short line land survey measurements.

Today, GPS receivers are routinely being used to conduct all types of land and geodetic control surveys, and to precisely position photo-aircraft to reduce the amount of ground control needed for mapping.

The nonsurveyor civilian uses of GPS outnumber the survey uses of the system. One of the major uses of GPS is for fleet management and control. Several cities have equipped emergency vehicles with receivers and computers with screens that display the cities' road system. The location of each emergency vehicle can be sent to a dispatcher by radio link so that disposition of the resources are known, and vehicles can be rerouted when necessary. Similar systems are used to track trains and freight hauling vehicles. Probably, all aircraft and vessels will be equipped with GPS in the near future.

GPS is also being used by hikers and boaters to determine their locations. Some manufacturers are presently offering a combined system of GPS and computer graphics for use in automobiles at the cost of a good high-fidelity music system.

2.4.2 Receiver types

The uses of GPS described in the previous section are just a sample of the applications of this system. The diversity of the uses is matched by the type of receivers available today. This section will give an overview of the equipment marketed today; however, more details will be provided in Sect. 5.2. Based on the type of observables (i.e., code pseudoranges or carrier phases) and on the availability of codes (i.e., C/A-code, P-code, or Y-code), one can classify GPS receivers into four groups: (1) C/A-code pseudorange, (2) C/A-code carrier phase, (3) P-code carrier phase, and (4) Y-code carrier phase measuring instruments.

C/A-code pseudorange receivers
With this type of receiver, only code pseudoranges using the C/A-code are

measured. The receiver is usually a hand-held device powered by flashlight batteries. Typical devices output the three-dimensional position either in longitude, latitude, and height or in some map projection system (e.g., UTM coordinates and height). Receivers with four or more channels are preferred for applications where the receiver is in motion since simultaneous satellite ranges can be measured to produce more accurate positions. On the other hand, a single channel receiver would still be adequate for applications where the receiver is at a fixed location and the range measurements can be sequentially determined. The basic multichannel C/A-code pseudorange receiver is the type of receiver that is mostly used by hikers, boaters, and in automobiles.

C/A-code carrier receivers
With this type of receiver, code ranges and carrier phases from the L1 carrier only are obtained because the C/A-code is not modulated on L2. This means that no dual frequency data are available.

Most of the receivers for surveying in the early stage of GPS used the C/A-code to acquire and lock on to the L1 carrier. Most instruments have a minimum of four independent receiver channels and some of the more recent designs have 12 channels. These receivers perform all the functions of the previously described models and, in addition, store the time-tagged code range and carrier phase in some type of memory. Early models used laptop computers and magnetic tapes to store the measured data. Later models store measurement data in memory chips and PCMCIA cards.

This type of receiver has been augmented to measure the phases of the L2 carrier by the use of some codeless technique. The drawback is that the signal-to-noise ratio (SNR) of the L2 measurements is considerably lower than the C/A-code measurements on L1. Normally, the L2 phase is used in combination with the L1 measurement to reduce the ionospheric effect on the signal and, thus, provide a more accurate vector determination (especially for long lines).

These receivers can be used for all types of precise surveys including static, kinematic, and pseudokinematic methods.

P-code receivers
This type of receiver uses the P-code and is able to lock on to the L1 and L2 carrier. In the absence of A-S, the observables are derived by first correlating the signals with a replica of the P-code. After removing the P-code from the received satellite signal, phase measurements can be performed. One of the first receivers for surveying, point positioning, and navigation was the P-code TI-4100 receiver, completed in 1984. This receiver was developed more

from a military perspective than a civilian one and only military-related development would have attempted this. Manufacturers of civilian receivers were able to justify P-code work around 1989–1990. In the fall of 1991, the two main advantages of the P-code receiver were demonstrated by another P-code receiver during FGCC tests. The first is its capability to measure long (100 km) lines to an accuracy of a few centimeters. The second advantage is that P-code instruments can measure moderate length lines (20 km) to an accuracy of a few millimeters with as little as some minutes of data using techniques based on a linear combination of the measured phases of L1 and L2.

With A-S activated, in the emitted signal the P-code is replaced by the unknown Y-code. Thus, traditional P-code correlation technique can no longer be applied. However, this type of receiver can operate in a codeless or quasi-codeless mode providing carrier phase data and code pseudoranges for the L2 frequency without knowledge of the Y-code. The L2 tracking is accomplished using four techniques which differ in their performance characteristics: signal squaring, cross correlation, code correlation followed by squaring, and the Z-tracking technique. More details on these techniques can be found in Sect. 5.2.

Y-code receivers
This type of receiver provides access to the P-code with A-S invoked. Thus, the code ranges and phases can be derived from L1 and L2 signals by the P-code correlation technique. The access to the P-code is achieved by installing Auxiliary Output Chips (AOC) in each receiver channel which allow the decryption of the Y-code. However, only users authorized by the DoD have access to the AOC.

2.4.3 Information services

Several governmental and private information services have been established to provide GPS status information and data to the civilian users. Generally, the information contains constellation status reports, scheduled outages, and the DoD Notice Advisories to Navstar Users (NANU). Orbital data are provided in the form of an almanac suitable for making GPS coverage and satellite visibility predictions, and as precise ephemerides suitable for making the most precise vector computations. General information is also provided by listing the various GPS papers and meetings.

The official source for civilian information is the Navigation Information Service (NIS), formerly the GPS Information Center. This service is run by the U.S. Coast Guard (USCG) and includes 24-hour operation of a

telephone information service. In the U.S., call (703) 313- to enter the service and dial the extension 5900 for live information, the extension 5907 for GPS status voice recording and the extension 5920 for FAX. Information by the USCG Navigation Center is also disseminated via Internet. The e-mail address reads webmaster@smtp.navcen.uscg.mil and the Uniform Resource Locator (URL) in the World Wide Web (WWW) is included in Table 2.2. More details can be found in Department of Defense and Department of Transportation (2000).

Comprehensive information including precise ephemerides, satellite clock parameters, and other data is provided by the Central Bureau Information System (CBIS) of the International GPS Service for Geodynamics (IGS) located at the U.S. Jet Propulsion Laboratory (JPL). The CBIS is accessible through Internet and offers file transfer capability by anonymous file transfer protocol (FTP). More details on the CBIS can be found in, e.g., Gurtner (1995).

Outside the U.S., GPS information sources are also available. Among them are: the Australian Surveying and Land Information Group (AUSLIG), the Canadian Space Geodesy Forum (CANSPACE), the German GPS Information and Observation System (GIBS), and the Russian Interstate Navigation Information Center (INIC) to name a few. The actual coordinates of the information services are published regularly, for example, in the monthly magazine *GPS World*. Some Internet addresses are given in Table 2.2 providing a variety of links to other GPS related sites in the Internet. These include links to manufacturers, associations, governments, and universities. Some of them offer also basic information or tutorials for novice GPS users. A comprehensive overview of such tutorials can be found on the Web site http://www.gpsy.com/gpsinfo.

Table 2.2. GPS information services

Agency	Location	WWW address
AUSLIG	Australia	http://www.auslig.gov.au
CBIS	U.S.	http://igscb.jpl.nasa.gov
GIBS	Germany	http://gibs.leipzig.ifag.de
NIS	U.S.	http://www.navcen.uscg.mil

3 Reference systems

3.1 Introduction

The basic equation which relates the range ϱ with the instantaneous position vector $\underline{\varrho}^S$ of a satellite and the position vector $\underline{\varrho}_R$ of the observing site reads

$$\varrho = \|\underline{\varrho}^S - \underline{\varrho}_R\| \,. \tag{3.1}$$

In Eq. (3.1), both vectors must be expressed in a uniform coordinate system. The definition of a three-dimensional Cartesian system requires a convention for the orientation of the axes and for the location of the origin.

For global applications such as satellite geodesy, equatorial coordinate systems are appropriate. According to Fig. 3.1, a space-fixed or celestial system $\underline{X}_i^0$ and an earth-fixed or terrestrial system $\underline{X}_i$ must be distinguished where $i = 1, 2, 3$. The earth's rotational vector $\underline{\omega}_E$ serves as $\underline{X}_3$-axis in both cases. The $\underline{X}_1^0$-axis for the space-fixed system points towards the vernal equinox and is, thus, the intersection line between the equatorial and the ecliptic plane. The $\underline{X}_1$-axis of the earth-fixed system is defined by the intersection line of the equatorial plane with the plane represented by the Greenwich meridian. The angle Θ_0 between the two systems is called Greenwich sidereal time. The $\underline{X}_2$-axis being orthogonal to both the $\underline{X}_1$-axis and the $\underline{X}_3$-axis completes a right-handed coordinate frame.

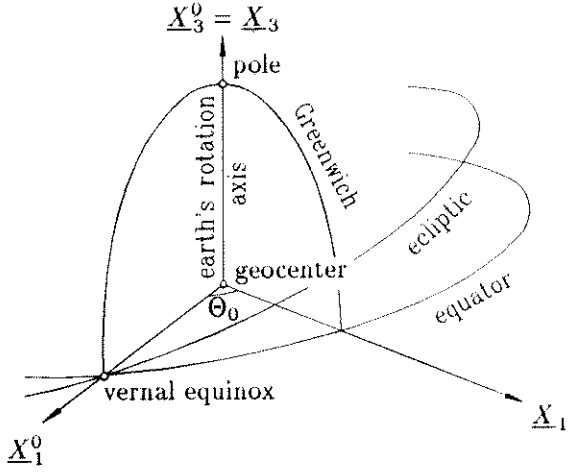

Fig. 3.1. Equatorial coordinate systems

6 Observables

6.1 Data acquisition

In concept, the GPS observables are ranges which are deduced from measured time or phase differences based on a comparison between received signals and receiver generated signals. Unlike the terrestrial electronic distance measurements, GPS uses the "one way concept" where two clocks are used, namely one in the satellite and the other in the receiver. Thus, the ranges are biased by satellite and receiver clock errors and, consequently, they are denoted as pseudoranges.

6.1.1 Code pseudoranges

Let us denote by t^S the reading of the satellite clock at emission time and by t_R the reading of the receiver clock at signal reception time. Analogously, the delays of the clocks with respect to GPS system time are termed δ^S and δ_R. Recall that the satellite clock reading t^S is transmitted via the PRN code. The difference between the clock readings is equivalent to the time shift Δt which aligns the satellite and reference signal during the code correlation procedure in the receiver. Thus,

$$\begin{aligned} \Delta t = t_R - t^S &= [t_R(\mathrm{GPS}) + \delta_R] - [t^S(\mathrm{GPS}) + \delta^S] \\ &= \Delta t(\mathrm{GPS}) + \Delta\delta\,, \end{aligned} \tag{6.1}$$

where $\Delta t(\mathrm{GPS}) = t_R(\mathrm{GPS}) - t^S(\mathrm{GPS})$ and $\Delta\delta = \delta_R - \delta^S$. The bias δ^S of the satellite clock can be modeled by a polynomial with the coefficients being transmitted in the first subframe of the navigation message. Assuming the δ^S correction is applied, $\Delta\delta$ equals the receiver clock delay. The time interval Δt multiplied by the speed of light c yields the pseudorange R and, hence,

$$R = c\,\Delta t = c\,\Delta t(\mathrm{GPS}) + c\,\Delta\delta = \varrho + c\,\Delta\delta\,. \tag{6.2}$$

Note that the C/A-code repeats every millisecond which corresponds to 300 km in range. Since the satellites are at a distance of about 20 000 km from the earth, C/A-code pseudoranges are ambiguous. However, this ambiguity can be easily resolved during initial satellite acquisition by introducing approximate (within some few hundred kilometers) position coordinates of the receiver (Lachapelle 1991).

The range ϱ is calculated from the true signal travel time. In other words, ϱ corresponds to the distance between the position of the satellite at epoch t^S(GPS) and the position of the antenna of the receiver at epoch t_R(GPS). Since ϱ is a function of two different epochs, it is often expanded into a Taylor series with respect to, e.g., the emission time

$$\begin{aligned} \varrho = \varrho(t^S, t_R) &= \varrho(t^S, (t^S + \Delta t)) \\ &= \varrho(t^S) + \dot{\varrho}(t^S)\,\Delta t \end{aligned} \tag{6.3}$$

where $\dot{\varrho}$ denotes the time derivative of ϱ or the radial velocity of the satellite relative to the receiving antenna. All epochs in Eq. (6.3) are expressed in GPS system time.

The maximum radial velocity for GPS satellites in the case of a stationary receiver is $\dot{\varrho} \approx 0.9\,\mathrm{km\,s^{-1}}$, and the travel time of the satellite signal is about 0.07 s. The correction term in Eq. (6.3), thus, amounts to some 60 m.

The precision of a pseudorange derived from code measurements has been traditionally about 1% of the chip length. Thus, a precision of roughly 3 m and 0.3 m is achieved with C/A-code and P-code pseudoranges respectively. However, recent developments demonstrate that a precision of about 0.1% of the chip length is possible.

6.1.2 Phase pseudoranges

Let us denote by $\varphi^S(t)$ the phase of the received and reconstructed carrier with frequency f^S and by $\varphi_R(t)$ the phase of a reference carrier generated in the receiver with frequency f_R. Here, the parameter t is an epoch in the GPS time system reckoned from an initial epoch $t_0 = 0$. According to Eq. (5.5), the following phase equations are obtained

$$\begin{aligned} \varphi^S(t) &= f^S t - f^S \frac{\varrho}{c} - \varphi_0^S \\ \varphi_R(t) &= f_R t - \varphi_{0R}\,. \end{aligned} \tag{6.4}$$

The initial phases φ_0^S, φ_{0R} are caused by clock errors and are equal to

$$\begin{aligned} \varphi_0^S &= -f^S \delta^S \\ \varphi_{0R} &= -f_R \delta_R\,. \end{aligned} \tag{6.5}$$

Hence, the beat phase $\varphi_R^S(t)$ is given by

$$\begin{aligned} \varphi_R^S(t) &= \varphi^S(t) - \varphi_R(t) \\ &= -f^S \frac{\varrho}{c} + f^S \delta^S - f_R \delta_R + (f^S - f_R)\, t\,. \end{aligned} \tag{6.6}$$

The deviation of the frequencies f^S, f_R from the nominal frequency f is only in the order of some fractional parts of Hz. This may be verified by considering, e.g., a short-time stability in the frequencies of $df/f = 10^{-12}$. With the nominal carrier frequency $f \approx 1.5\,\mathrm{GHz}$, the frequency error, thus, becomes $df = 1.5 \cdot 10^{-3}\,\mathrm{Hz}$. Such a frequency error may be neglected because during signal propagation (i.e., $t = 0.07$ seconds) a maximum error of 10^{-4} cycles in the beat phase is generated which is below the noise level. The clock errors are in the range of milliseconds and are, thus, less effective. Summarizing, Eq. (6.6) may be written in the simplified form

$$\varphi_R^S(t) = -f \frac{\varrho}{c} - f\,\Delta\delta \tag{6.7}$$

where again $\Delta\delta = \delta_R - \delta^S$ has been introduced. If the assumption of frequency stability is incorrect and the oscillators are unstable, then their behavior has to be modeled by, for example, polynomials where clock and frequency offsets and a frequency drift are determined. A complete carrier phase model which includes the solution of large (e.g., 1 second) receiver clock errors was developed by Remondi (1984). Adequate formulas can also be found in King et al. (1987), p. 55. No further details are given here because in practice eventual residual errors will be eliminated by differencing the measurements.

Switching on a receiver at epoch t_0, the instantaneous fractional beat phase is measured. The initial integer number N of cycles between satellite and receiver is unknown. However, when tracking is continued without loss of lock, the number N, also called integer ambiguity, remains the same and the beat phase at epoch t is given by

$$\varphi_R^S(t) = \Delta\varphi_R^S \Big|_{t_0}^{t} + N \tag{6.8}$$

where $\Delta\varphi_R^S$ denotes the (measurable) fractional phase at epoch t augmented by the number of integer cycles since the initial epoch t_0. A geometrical interpretation of Eq. (6.8) is provided in Fig. 6.1 where $\Delta\varphi_i$ is a shortened notation for $\Delta\varphi_R^S \,|_{t_0}^{t_i}$ and, for simplicity, the initial fractional beat phase $\Delta\varphi_0$ is assumed to be zero. Substituting Eq. (6.8) into Eq. (6.7) and denoting the negative observation quantity by $\Phi = -\Delta\varphi_R^S$ yields the equation for the phase pseudoranges

$$\Phi = \frac{1}{\lambda}\varrho + \frac{c}{\lambda}\Delta\delta + N \tag{6.9}$$

where the wavelength λ has been introduced according to Eq. (5.2). Multiplying the above equation by λ scales the phase expressed in cycles to a range which only differs from the code pseudorange by the integer multiples

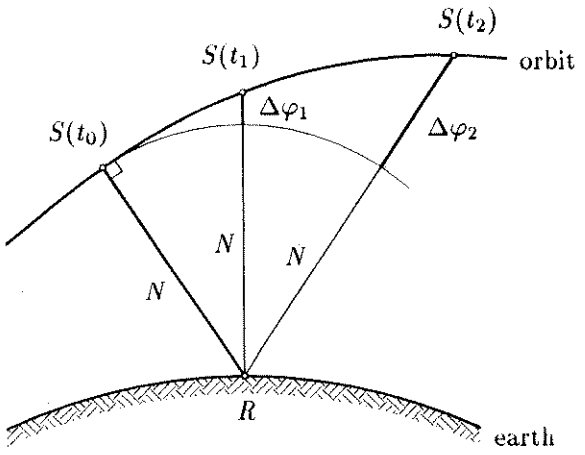

Fig. 6.1. Geometrical interpretation of phase range

of λ. Again, the range ϱ represents the distance between the satellite at emission epoch t and the receiver at reception epoch $t + \Delta t$. The phase of the carrier can be measured to better than 0.01 cycles which corresponds to millimeter precision.

It should be noted that a plus sign convention has been chosen for Eq. (6.9). This choice is somewhat arbitrary since quite often the phase Φ and the distance ϱ have different signs. Actually, the sign is receiver dependent because the beat phase is generated in the receiver and the combination of the satellite and the receiver signal differs for various receiver types.

6.1.3 Doppler data

Some of the first solution models proposed for GPS were to use the Doppler observable as with the TRANSIT system. This system used the integrated Doppler shifts (i.e., phase differences) which were scaled to delta ranges. The raw Doppler shift, cf. Eq. (5.6), being linearly dependent on the radial velocity and, thus, allowing for velocity determination in real time is important for navigation. Considering Eq. (6.9), the equation for the observed Doppler shift scaled to range rate is given by

$$D = \lambda \dot{\Phi} = \dot{\varrho} + c\,\Delta\dot{\delta} \tag{6.10}$$

where the derivatives with respect to time are indicated by a dot. The raw Doppler shift is less accurate than integrated Doppler. An estimate of the

achievable accuracy is 0.001 Hz. This corresponds to $0.3\,\mathrm{m\,s^{-1}}$ if the Doppler shift is measured in the C/A-code tracking loop.

A detailed derivation of Doppler equations within the frame of GPS is given in Remondi (1984) where even relativistic effects are accounted for. It is worth noting here that the raw Doppler shift is also applied to determine integer ambiguities in kinematic surveying (Remondi 1991a) or is used as an additional independent observable for point positioning.

6.1.4 Biases and noise

The code pseudoranges, cf. Eq. (6.2), and phase pseudoranges, cf. Eq. (6.9), are affected by both, systematic errors or biases and random noise. Note that Doppler measurements are affected by the bias rates only. The error sources can be classified into three groups, namely satellite related errors, propagation medium related errors, and receiver related errors. Some range biases are listed in Table 6.1.

Some of the systematic errors can be modeled and give rise to additional terms in the observation equations which will be explained in detail in subsequent sections. As mentioned earlier, systematic effects can also be eliminated by appropriate combinations of the observables. Differencing between receivers eliminates satellite-specific biases, and differencing between satellites eliminates receiver-specific biases. Thus, double-differenced pseudoranges are, to a high degree, free of systematic errors originating from the satellites and from the receivers. With respect to refraction, this is only true for short baselines where the measured ranges at both endpoints are affected equally. In addition, ionospheric refraction can be virtually eliminated by an adequate combination of dual frequency data. Antenna phase center variations are treated in Sect. 6.5. Multipath is caused by multiple reflections

Table 6.1. Range biases

Source	Effect
Satellite	Clock bias
	Orbital errors
Signal propagation	Ionospheric refraction
	Tropospheric refraction
Receiver	Antenna phase center variation
	Clock bias
	Multipath

of the signal (which can also occur at the satellite during signal emission). The interference between the direct and the reflected signal is largely not random; however, it may also appear as a noise. Wells et al. (1987) report a similar effect called imaging where a reflecting obstacle generates an image of the real antenna which distorts the antenna pattern. Both effects, multipath and imaging, can be considerably reduced by selecting sites protected from reflections (buildings, vehicles, trees, etc.) and by an appropriate antenna design. It should be noted that multipath is frequency dependent. Therefore, carrier phases are less affected than code ranges (Lachapelle 1990). More details on the multipath problems are given in Sect. 6.6.

The random noise mainly contains the actual observation noise plus random constituents of multipath (especially for kinematic applications). The pseudorange noise is summarized in Table 6.2.

The measurement noise, an estimation of the satellite biases, and the contributions from the wave propagation are combined in the User Equivalent Range Error (UERE). This UERE is transmitted via the navigation message. In combination with a DOP factor, explained in Sect. 9.6, UERE allows for an estimation of the achievable point positioning accuracy.

Table 6.2. Range noise

Range	Noise
Code range (C/A-code)	10–300 cm
Code range (P-code)	10–30 cm
Phase range	0.2–5 mm

6.2 Data combinations

GPS observables are obtained from the code information or the carrier wave in the broadcast satellite signal. Recall that the P-code is modulated on both carriers L1 and L2, whereas the C/A-code is modulated on L1 only. Consequently, one could measure the code ranges R_{L1}, R_{L2}, the carrier phases Φ_{L1}, Φ_{L2}, and the corresponding Doppler shifts D_{L1}, D_{L2} for a single epoch. Note that the L1 observables may either be derived from the C/A-code or from the P-code. In general, not all observables are available because, for example, a single frequency receiver delivers only data from the L1 frequency. Furthermore, the Doppler observables are not considered here.

The objectives of this section are to show how linear combinations are developed for dual frequency data, and how code range smoothing by means of carrier phases is performed.

6.2.1 Linear phase combinations

General remarks

The linear combination of two phases φ_1 and φ_2 is defined by

$$\varphi = n_1 \varphi_1 + n_2 \varphi_2 \tag{6.11}$$

where n_1 and n_2 are arbitrary numbers. The substitution of the relations $\varphi_i = f_i t$ for the corresponding frequencies f_1 and f_2 gives

$$\varphi = n_1 f_1 t + n_2 f_2 t = f t\,. \tag{6.12}$$

Therefore,

$$f = n_1 f_1 + n_2 f_2 \tag{6.13}$$

is the frequency and

$$\lambda = \frac{c}{f} \tag{6.14}$$

is the wavelength of the linear combination.

Considering a certain noise level for the phases, the noise level increases for the linear combination. Applying the error propagation law and assuming the same noise for both phases, the noise of the linear combination is amplified by the factor $\sqrt{n_1^2 + n_2^2}$ compared to the noise of a single phase. To compute this factor correctly, proper noise levels must be taken into account.

Linear combinations with integer numbers

In the case of GPS, the simplest nontrivial linear combinations of L1 and L2 carrier phases Φ_{L1} and Φ_{L2} in Eq. (6.11) are $n_1 = n_2 = 1$, yielding the sum

$$\Phi_{L1+L2} = \Phi_{L1} + \Phi_{L2} \tag{6.15}$$

and $n_1 = 1$, $n_2 = -1$, leading to the difference

$$\Phi_{L1-L2} = \Phi_{L1} - \Phi_{L2}\,. \tag{6.16}$$

The corresponding wavelengths according to (6.13) and (6.14) are

$$\begin{aligned} \lambda_{L1+L2} &= 10.7 \text{ cm} \\ \lambda_{L1-L2} &= 86.2 \text{ cm} \end{aligned} \tag{6.17}$$

where the numerical values for the carrier frequencies f_{L1} and f_{L2} (Table 5.2) have been substituted. The combination Φ_{L1+L2} is denoted as narrow lane and Φ_{L1-L2} as wide lane. The lane signals are applied for ambiguity resolution (Sect. 9.2).

The advantage of a linear combination with integer numbers is that the integer nature of the ambiguities is preserved.

Linear combinations with real numbers
A slightly more complicated linear combination results from the choice

$$n_1 = 1 \qquad n_2 = -\frac{f_{L2}}{f_{L1}} \tag{6.18}$$

leading to the combination

$$\Phi_{L1,L2} = \Phi_{L1} - \frac{f_{L2}}{f_{L1}} \Phi_{L2} \tag{6.19}$$

which is frequently denoted as geometric residual. This quantity is the kernel in a combination used to reduce ionospheric effects (Sect. 6.3.2).

Another linear combination follows from the reciprocal values of (6.18)

$$n_1 = 1 \qquad n_2 = -\frac{f_{L1}}{f_{L2}} \tag{6.20}$$

leading to the combination

$$\Phi_{L1,L2} = \Phi_{L1} - \frac{f_{L1}}{f_{L2}} \Phi_{L2} \tag{6.21}$$

which is frequently denoted as ionospheric residual. This quantity is used in the context of cycle slip detection (Sect. 9.1.2).

The drawback of a linear combination with real numbers is that the integer nature of the ambiguity is lost.

6.2.2 Code pseudorange smoothing

The objective here is to show the principle of code pseudorange smoothing by means of phase pseudoranges. This is an important issue in accurate real-time positioning.

Assuming dual frequency measurements for epoch t_1, the code pseudoranges $R_{L1}(t_1)$, $R_{L2}(t_1)$ and the carrier phase pseudoranges $\Phi_{L1}(t_1)$, $\Phi_{L2}(t_1)$ are obtained. Further assume, the code pseudoranges are scaled to cycles

(but still denoted as R) by dividing them by the corresponding carrier wavelength. Using the two frequencies f_{L1}, f_{L2}, the combination

$$R(t_1) = \frac{f_{L1}\, R_{L1}(t_1) - f_{L2}\, R_{L2}(t_1)}{f_{L1} + f_{L2}} \tag{6.22}$$

is formed for the code pseudoranges and the wide lane signal

$$\Phi(t_1) = \Phi_{L1}(t_1) - \Phi_{L2}(t_1) \tag{6.23}$$

for the carrier phase pseudoranges. From Eq. (6.22) one can see that the noise of the combined code pseudorange $R(t_1)$ is reduced by a factor of 0.7 compared to the noise of the single code measurement. The increase of the noise in the wide lane signal by a factor of $\sqrt{2}$ has no effect because the noise of the carrier phase pseudoranges is essentially lower than the noise of the code pseudoranges. Note that both signals $R(t_1)$ and $\Phi(t_1)$ have the same frequency and, thus, the same wavelength as may be verified by applying Eq. (6.13).

Combinations (6.22) and (6.23) are formed for each epoch. Additionally, for all epochs t_i after t_1, extrapolated values of the code pseudoranges $R(t_i)_{ex}$ can be calculated from

$$R(t_i)_{ex} = R(t_1) + (\Phi(t_i) - \Phi(t_1))\,. \tag{6.24}$$

The smoothed value $R(t_i)_{sm}$ is finally obtained by the arithmetic mean

$$R(t_i)_{sm} = \tfrac{1}{2}\,(R(t_i) + R(t_i)_{ex})\,. \tag{6.25}$$

Generalizing the above formulas for an arbitrary epoch t_i (with the preceding epoch t_{i-1}), a recursive algorithm is given by

$$\begin{aligned}
R(t_i) &= \frac{f_{L1}\, R_{L1}(t_i) - f_{L2}\, R_{L2}(t_i)}{f_{L1} + f_{L2}} \\
\Phi(t_i) &= \Phi_{L1}(t_i) - \Phi_{L2}(t_i) \\
R(t_i)_{ex} &= R(t_{i-1})_{sm} + (\Phi(t_i) - \Phi(t_{i-1})) \\
R(t_i)_{sm} &= \tfrac{1}{2}\,(R(t_i) + R(t_i)_{ex})
\end{aligned}$$

which works under the initial condition $R(t_1) = R(t_1)_{ex} = R(t_1)_{sm}$ for all $i > 1$.

The above algorithm assumes the data are free of gross errors. However, carrier phase data are sensitive to changes in the integer ambiguity (i.e., cycle slips). To circumvent this problem, a variation of the algorithm is

subsequently given. Using the same notations as before for an epoch t_i, the smoothed code pseudorange is obtained by

$$R(t_i)_{\mathrm{sm}} = w\,R(t_i) + (1-w)\,(R(t_{i-1})_{\mathrm{sm}} + \Phi(t_i) - \Phi(t_{i-1})) \qquad (6.26)$$

where w is a time dependent weight factor. For the first epoch $i = 1$, the weight is set $w = 1$; thus, putting the full weight on the measured code pseudorange. For consecutive epochs, the weight of the code phase is continuously reduced and, thus, emphasizes the influence of the carrier phases. A reduction of the weight by 0.01 from epoch to epoch was tested in a kinematic experiment with a data sampling rate of 1 Hz. After 100 seconds, only the smoothed value of the previous epoch (augmented by the carrier phase difference) is taken into account. Again, in the case of cycle slips, the algorithm would fail. A simple check of the carrier phase difference for two consecutive epochs by the Doppler shift multiplied by the time interval may detect data irregularities such as cycle slips. After the occurrence of a cycle slip, the weight is reset to $w = 1$ which fully eliminates the influence of the erroneous carrier phase data. The key of this approach is that cycle slips must be detected but do not have to be corrected.

Another smoothing algorithm for code pseudoranges uses phase differences $\Delta\Phi(t_i, t_1)$ obtained by the integrated Doppler shift between the current epoch t_i and the starting epoch t_1. Note that the integrated Doppler shifts are insensitive to cycle slips. From each code pseudorange $R(t_i)$ at epoch t_i, an estimate of the code pseudorange at epoch t_1 can be given by

$$R(t_1)_i = R(t_i) - \Delta\Phi(t_i, t_1) \qquad (6.27)$$

where the subscript i on the left side of the equation indicates the epoch that the code pseudorange $R(t_1)$ is computed from. Obtaining an estimate consecutively for each epoch, the arithmetic mean $R(t_1)_{\mathrm{m}}$ of the code pseudorange for n epochs is calculated by

$$R(t_1)_{\mathrm{m}} = \frac{1}{n}\sum_{i=1}^{n} R(t_1)_i \qquad (6.28)$$

and the smoothed code pseudorange for an arbitrary epoch results from

$$R(t_i)_{\mathrm{sm}} = R(t_1)_{\mathrm{m}} + \Delta\Phi(t_i, t_1)\,. \qquad (6.29)$$

The advantage of this procedure lies in the reduction of the noise in the initial code pseudorange by averaging an arbitrary number n of measured code pseudoranges. Note from the three formulas (6.27) through (6.29) that the algorithm may also be applied successively epoch by epoch where the

arithmetic mean must be updated from epoch to epoch. Using the above notations, formula (6.29) also works for epoch t_1, where, of course, $\Delta\Phi(t_1, t_1)$ is zero and there is no smoothing effect.

All the smoothing algorithms are also applicable if only single frequency data are available. In this case, $R(t_i)$, $\Phi(t_i)$, and $\Delta\Phi(t_i, t_1)$ denote the single frequency code pseudorange, carrier phase pseudorange, and phase difference respectively.

6.3 Atmospheric effects

6.3.1 Phase and group velocity

Consider a single electromagnetic wave propagating in space with wavelength λ and frequency f. The velocity of its phase

$$v_{\mathrm{ph}} = \lambda\, f \qquad (6.30)$$

is denoted phase velocity. For GPS, the carrier waves L1 and L2 are propagating with this velocity.

For a group of waves with slightly different frequencies, the propagation of the resultant energy is defined by the group velocity

$$v_{\mathrm{gr}} = -\frac{df}{d\lambda}\,\lambda^2 \qquad (6.31)$$

according to Bauer (1994), p. 96. This velocity has to be considered for GPS code measurements.

A relation between phase and group velocity may be derived by forming the total differential of Eq. (6.30) resulting in

$$dv_{\mathrm{ph}} = f\,d\lambda + \lambda\,df \qquad (6.32)$$

which can be rearranged to

$$\frac{df}{d\lambda} = \frac{1}{\lambda}\,\frac{dv_{\mathrm{ph}}}{d\lambda} - \frac{f}{\lambda}\,. \qquad (6.33)$$

The substitution of (6.33) into (6.31) yields

$$v_{\mathrm{gr}} = -\lambda\,\frac{dv_{\mathrm{ph}}}{d\lambda} + f\,\lambda \qquad (6.34)$$

or finally the Rayleigh equation

$$v_{\mathrm{gr}} = v_{\mathrm{ph}} - \lambda\,\frac{dv_{\mathrm{ph}}}{d\lambda}\,. \qquad (6.35)$$

4. A description of the instrumentation used should include both the GPS equipment and conventional equipment along with serial numbers. An explanation of how the tribrachs or bipods were tested for plumb should be given. If survey towers or special range poles were used, their use should be described with an explanation of how the antenna was collimated.
5. The computation scheme for the project should be described including which version of the processing software was used and which least squares adjustment was applied. An exhibit such as Table 7.8 is particularly useful in visualizing how the survey was conducted. The satellites tracked during each session should be included in this listing or in a separate exhibit. Also, an exhibit such as Table 7.9 should be included to show the quality factors for each line. The inclusion of abstracts of each vector would also be helpful.
6. The computation of coordinates for all eccentric points should be included. In the case of horizontal points, sketches and the direct computation results should be shown. For vertical points, a copy of the level records should be included in an appendix.
7. All problems encountered should be discussed and equipment failures listed. Unusual solar activity should be mentioned as well as multipath problems and other factors affecting the survey.
8. The following lists should be included in the report:
   - list of loop closures,
   - occupation schedule (e.g., Table 7.8),
   - vector statistics (e.g., Table 7.9),
   - free least squares adjustment,
   - portion of fixed adjustment showing rotation angles and statistics,
   - list of adjusted positions and plane coordinates,
   - project statistics,
   - copies of "original" site occupation logs,
   - equipment malfunction log,
   - project sketch showing all points and control with a title box, scale, and projection tic marks.
9. Finally, a copy of the original observations (or translated RINEX) should be transmitted as part of the survey. Copies of the adjustment input file and vector output files would be advantageous.

When surveys are properly performed and documented, they provide a lasting contribution to the profession. Often, data can be used in later years by others to study a particular phenomenon or the work may be included in a larger project. Proper use of measurements can only be made when the survey is thoroughly documented for posterity.

8 Mathematical models for positioning

8.1 Point positioning

8.1.1 Point positioning with code ranges

Code range model

The code pseudorange at an epoch t can be modeled, cf. Eq. (6.2), by

$$R_i^j(t) = \varrho_i^j(t) + c\,\Delta\delta_i^j(t)\,. \tag{8.1}$$

Here, $R_i^j(t)$ is the measured code pseudorange between the observing site i and the satellite j, $\varrho_i^j(t)$ is the geometric distance between the satellite and the observing point, and c is the speed of light. The last item to be explained is $\Delta\delta_i^j(t)$. This clock bias represents the combined clock offsets of the receiver and the satellite clock with respect to GPS time, cf. Eq. (6.1).

Examining Eq. (8.1), the desired point coordinates to be determined are implicit in the distance $\varrho_i^j(t)$, which can explicitly be written as

$$\varrho_i^j(t) = \sqrt{(X^j(t) - X_i)^2 + (Y^j(t) - Y_i)^2 + (Z^j(t) - Z_i)^2} \tag{8.2}$$

where $X^j(t)$, $Y^j(t)$, $Z^j(t)$ are the components of the geocentric position vector of the satellite at epoch t, and X_i, Y_i, Z_i are the three unknown ECEF coordinates of the observing site. Now, the clock bias $\Delta\delta_i^j(t)$ must be investigated in more detail. For the moment consider a single epoch; a single position i is automatically implied. Each satellite contributes one unknown clock bias which can be recognized from the superscript j at the clock term. Neglecting, for the present, the site i clock bias, the pseudorange equation for the first satellite would have four unknowns. These are the three site coordinates and one clock bias of this satellite. Each additional satellite adds one equation with the same site coordinates but with a new satellite clock bias. Thus, there would always be more unknowns than measurements. Even when an additional epoch is considered, new satellite clock biases must be modeled due to clock drift. Fortunately, the satellite clock information is known and transmitted via the broadcast navigation message in the form of three polynomial coefficients a_0, a_1, a_2 with a reference time t_c. Therefore the equation

$$\delta^j(t) = a_0 + a_1(t - t_c) + a_2(t - t_c)^2 \tag{8.3}$$

enables the calculation of the satellite clock bias at epoch t. It should be noted that the polynomial (8.3) removes a great deal of the satellite clock bias, but a small amount of error remains.

The combined bias term $\Delta\delta_i^j(t)$ is split into two parts by

$$\Delta\delta_i^j(t) = \delta_i(t) - \delta^j(t) \tag{8.4}$$

where the satellite related part is known by (8.3) and the receiver related term $\delta_i(t)$ remains unknown. Substituting (8.4) into (8.1) and shifting the satellite clock bias to the left side of the equation yields

$$R_i^j(t) + c\,\delta^j(t) = \varrho_i^j(t) + c\,\delta_i(t)\,. \tag{8.5}$$

Note that the left side of the equation contains observed or known quantities, while the terms on the right side are unknown.

Basic configurations

Basic configurations are defined by the condition that the number of observations must be equal to or greater than the number of unknowns. This condition is sufficient but does not necessarily give a solution. The reason for this is that inherent rank deficiencies may prevent a numerical solution because of a singularity. More explanations are given later when the rank deficiency becomes an issue.

The number of observations is $n_j\,n_t$ where n_j denotes the number of satellites and n_t the number of epochs.

For static point positioning, the three coordinates of the observing site and the receiver clock bias for each observation epoch are unknown. Thus, the number of unknowns is $3 + n_t$. The basic configuration is defined by

$$n_j\,n_t \geq 3 + n_t \tag{8.6}$$

which yields the explicit relation

$$n_t \geq \frac{3}{n_j - 1}\,. \tag{8.7}$$

The minimum number of satellites to get a solution is $n_j = 2$ leading to $n_t \geq 3$ observation epochs. For $n_j = 4$, the solution $n_t \geq 1$ is obtained. This solution reflects the instantaneous positioning capability of GPS, where the four unknowns at any epoch are solved if at least four satellites can be tracked.

For kinematic point positioning, the basic configuration can be directly derived from the following consideration. Due to the motion of the receiver,

the number of the unknown station coordinates is $3n_t$. Adding the n_t unknown receiver clock biases, the total number of unknowns is $4n_t$. Hence, the basic configuration is defined by Eq. (8.6),

$$n_j\,n_t \geq 4n_t \tag{8.8}$$

yielding $n_j \geq 4$. In other words, the position (and velocity) of a moving receiver can be determined at any instant as long as at least four satellites are tracked. Geometrically, the solution is represented by the intersection of four pseudoranges. For the rigorous analytical solution see Kleusberg (1994), Lichtenegger (1995).

The basic configurations must be considered from a theoretical point of view. The solution $n_j = 2$, $n_t \geq 3$ for static point positioning, for example, means that simultaneous observations of two satellites over three epochs would theoretically suffice. In practice, however, this situation would yield unacceptable results or the computation would fail because of an ill-conditioned system of observation equations unless the epochs were widely spaced (e.g., hours). A solution is also possible if observations of three epochs for two satellites are made, followed by three additional epochs (e.g., seconds apart) for two other satellites. Such an application will be rare but is imaginable under special circumstances (e.g., in urban areas).

8.1.2 Point positioning with carrier phases

Phase range model

Pseudoranges can also be obtained from carrier phase measurements. The mathematical model for these measurements, cf. Eq. (6.9), is given by

$$\Phi_i^j(t) = \frac{1}{\lambda}\,\varrho_i^j(t) + N_i^j + f^j\,\Delta\delta_i^j(t) \tag{8.9}$$

where $\Phi_i^j(t)$ is the measured carrier phase expressed in cycles, λ is the wavelength, and $\varrho_i^j(t)$ is the same as for the code range model. The time independent phase ambiguity N_i^j is an integer number and, therefore, often called integer ambiguity or integer unknown or simply ambiguity. The term f^j denotes the frequency of the satellite signal, and $\Delta\delta_i^j(t)$ is the combined receiver and satellite clock bias.

Substituting Eq. (8.4) into Eq. (8.9) and shifting the satellite clock bias, known from Eq. (8.3), to the left side of the equation yields

$$\Phi_i^j(t) + f^j\,\delta^j(t) = \frac{1}{\lambda}\,\varrho_i^j(t) + N_i^j + f^j\,\delta_i(t)\,. \tag{8.10}$$

Basic configurations

Using the same notations as before, the number of observations is again

$n_j\, n_t$. The number of unknowns, however, is increased by the number n_j because of the ambiguities.

For static point positioning, the number of unknowns is composed of 3 coordinates of the observing station, n_j unknown ambiguities, and n_t unknown receiver clock biases. Referring to (8.10), the problem of the rank deficiency is encountered. Mathematically less interested readers may skip the next paragraph.

A few basics on rank and rank deficiency are given here. Deeper insight may be obtained from Koch (1987), Sects. 132, 333. Assume a large number of equations of type (8.10) being prepared to be solved for the unknowns. This implies a matrix-vector representation where the right side is composed of a product of a design matrix $\underline{A}$ and a vector comprising the unknowns in linear form. The rank of the design matrix is equal to the order of the largest nonsingular matrix that can be formed inside $\underline{A}$. Formulated differently: the maximum number of the linearly independent rows of matrix $\underline{A}$ is called the rank r of the matrix and is denoted by $r = \operatorname{rank} \underline{A}$. Linear dependence of two rows means that their linear combination yields a zero vector. The word rows in this definition may also be replaced by the word columns. For a simpler discussion, assume a quadratic matrix with $m \times m$ rows and columns. Thus, if the largest nonsingular matrix is the matrix $\underline{A}$ itself, the rank equals $r = \operatorname{rank} \underline{A} = m$ and the matrix is regular, i.e., it may be inverted without troubles. On the other hand, if the largest nonsingular matrix inside $\underline{A}$ is a matrix with, e.g., $(m-2) \times (m-2)$ rows and columns, the rank would be $r = m - 2$ and implies a rank deficiency of $m - r$ which turns out to be $m - (m-2)$ which amounts to 2. As a consequence, the singular system becomes regularly solvable if two unknowns (also denoted as parameters) are arbitrarily chosen. This equals the "fixing" of two parameters. Figuratively speaking, two of the parameters may be transferred to the left side of the matrix-vector system comprising the measurements. This transfer reduces on the other hand the columns of the matrix on the right side by the amount of the rank deficiency, i.e., in the example discussed by two. This concludes the short discussion on rank and rank deficiency.

The model in the form (8.10) comprises a rank deficiency of 1, this means that one of the unknown parameters may (and must) be arbitrarily chosen. Suppose that a receiver clock bias at one epoch is chosen, then, instead of n_t unknown receiver clock biases, only $n_t - 1$ clock biases remain. Therefore, the basic configuration for static point positioning without rank deficiency is defined by the relation

$$n_j\, n_t \geq 3 + n_j + (n_t - 1) \tag{8.11}$$

which yields explicitly the required number of epochs as

$$n_t \geq \frac{n_j + 2}{n_j - 1}\,. \tag{8.12}$$

The minimum number of satellites to get a solution is $n_j = 2$ leading to $n_t \geq 4$ observation epochs. Another integer solution pair is $n_j = 4$, $n_t \geq 2$.

For kinematic point positioning with phases, $3n_t$ unknown station coordinates must be considered because of the roving receiver compared to the 3 unknowns in (8.11). The other considerations including the discussion on the rank deficiency remain unchanged. Therefore, the basic configuration is defined by

$$n_j\, n_t \geq 3n_t + n_j + (n_t - 1) \tag{8.13}$$

yielding the explicit relation

$$n_t \geq \frac{n_j - 1}{n_j - 4}\,. \tag{8.14}$$

The minimum number of satellites to get a solution is $n_j = 5$ which have to be tracked for $n_t \geq 4$ epochs. Another integer solution pair is $n_j = 7$, $n_t \geq 2$.

Note that solutions for a single epoch (i.e., $n_t = 1$) do not exist for point positioning with carrier phases. As a consequence, kinematic point positioning with phases is only possible if the n_j phase ambiguities are known from some initialization. In this case, the phase range model converts to the code range model.

8.1.3 Point positioning with Doppler data

The mathematical model for Doppler data, cf. Eq. (6.10), is

$$D_i^j(t) = \dot{\varrho}_i^j(t) + c\,\Delta\dot{\delta}_i^j(t) \tag{8.15}$$

and may be considered as time derivative of a code or phase pseudorange. In this equation, $D_i^j(t)$ denotes the observed Doppler shift scaled to range rate, $\dot{\varrho}_i^j(t)$ is the instantaneous radial velocity between the satellite and the receiver, and $\Delta\dot{\delta}_i^j(t)$ is the time derivative of the combined clock bias term.

The radial velocity for a stationary receiver, cf. Eq. (4.45),

$$\dot{\varrho}_i^j(t) = \frac{\underline{\varrho}^j(t) - \underline{\varrho}_i}{\|\underline{\varrho}^j(t) - \underline{\varrho}_i\|} \cdot \dot{\underline{\varrho}}^j(t) \tag{8.16}$$

relates the unknown position vector $\underline{\varrho}_i$ of the receiver to the instantaneous position vector $\underline{\varrho}^j(t)$ and velocity vector $\dot{\underline{\varrho}}^j(t)$ of the satellite. These vectors

can be calculated from the satellite ephemerides. The contribution of the satellite clock to $\Delta\delta_i^j(t)$ is given by, cf. Eq. (8.3),

$$\dot{\delta}^j(t) = a_1 + 2a_2(t - t_c) \tag{8.17}$$

and is known. Summarizing, the observation equation (8.15) contains four unknowns. These unknowns are the three receiver coordinates $\underline{\varrho}_i$ and the receiver clock drift $\dot{\delta}_i(t)$. Hence, compared to the code range model, the Doppler equation contains the receiver clock drift instead of the receiver clock offset.

The concept of combined code pseudorange and Doppler data processing leads to a total of five unknowns. These unknowns are the three point coordinates, the receiver clock offset, and the receiver clock drift. Each satellite contributes two equations, one code pseudorange and one Doppler equation. Therefore, three satellites are sufficient to solve for the five unknowns.

The similarity of the pseudorange and the Doppler equation gives rise to the question of a linear dependence of the equations. However, it can be shown that the surfaces of constant pseudoranges and the surfaces of constant Doppler are orthogonal and hence independent (Levanon 1999).

8.2 Differential positioning

8.2.1 Basic concept

As shown in Sect. 7.1.2, differential positioning with GPS, abbreviated by DGPS, is a real-time positioning technique where two or more receivers are used. One receiver, usually at rest, is located at the reference or base station with known coordinates and the remote receivers are usually roving and their coordinates are to be determined. The reference station calculates pseudorange corrections (PRC) and range rate corrections (RRC) which are transmitted to the remote receiver in real time. The remote receiver applies the corrections to the measured pseudoranges and performs point positioning with the corrected pseudoranges. The use of the corrected pseudoranges improves the positional accuracy with respect to the base station.

8.2.2 DGPS with code ranges

Generalizing (8.5) and following Lichtenegger (1998), the code range at base station A to satellite j measured at epoch t_0 may be modeled by

$$R_A^j(t_0) = \varrho_A^j(t_0) + \Delta\varrho_A^j(t_0) + \Delta\varrho^j(t_0) + \Delta\varrho_A(t_0) \tag{8.18}$$

where $\varrho_A^j(t_0)$ is the geometric range, the term $\Delta\varrho_A^j(t_0)$ denotes range biases depending on the terrestrial base position and satellite position as well (e.g.,

radial orbital error, refraction effects), the range bias $\Delta\varrho^j(t_0)$ is purely satellite dependent (e.g., effect of satellite clock error), and the range bias $\Delta\varrho_A(t_0)$ is purely receiver dependent (e.g., effect of receiver clock error, multipath). Note that noise has been neglected in (8.18).

The pseudorange correction for satellite j at reference epoch t_0 is defined by the relation

$$\begin{aligned} \mathrm{PRC}^j(t_0) &= \varrho_A^j(t_0) - R_A^j(t_0) \\ &= -\Delta\varrho_A^j(t_0) - \Delta\varrho^j(t_0) - \Delta\varrho_A(t_0) \end{aligned} \tag{8.19}$$

and can be calculated since the geometric range $\varrho_A^j(t_0)$ is obtained from the known position of the reference station and the broadcast ephemerides and $R_A^j(t_0)$ is the measured quantity. In addition to the pseudorange correction $\mathrm{PRC}^j(t_0)$, the time derivative or range rate correction $\mathrm{RRC}^j(t_0)$ is determined at the base station.

Range and range rate corrections referring to the reference epoch t_0 are transmitted to the rover site B in real time. At B the pseudorange corrections are predicted for the observation epoch t using the relation

$$\mathrm{PRC}^j(t) = \mathrm{PRC}^j(t_0) + \mathrm{RRC}^j(t_0)(t - t_0) \tag{8.20}$$

where $t - t_0$ is defined as latency. The achievable accuracy increases for smaller variations of the pseudorange corrections and for smaller latencies.

Adapting (8.18) to the rover site B and epoch t, the code pseudorange measured at the rover can be modeled by

$$R_B^j(t) = \varrho_B^j(t) + \Delta\varrho_B^j(t) + \Delta\varrho^j(t) + \Delta\varrho_B(t)\,. \tag{8.21}$$

Applying the predicted pseudorange correction $\mathrm{PRC}^j(t)$, cf. Eq. (8.20), to the measured pseudorange $R_B^j(t)$ yields

$$R_B^j(t)_{\mathrm{corr}} = R_B^j(t) + \mathrm{PRC}^j(t) \tag{8.22}$$

or, after substitution of (8.21) and the pseudorange correction according to (8.19) and (8.20), respectively,

$$R_B^j(t)_{\mathrm{corr}} = \varrho_B^j(t) + [\Delta\varrho_B^j(t) - \Delta\varrho_A^j(t)] + [\Delta\varrho_B(t) - \Delta\varrho_A(t)] \tag{8.23}$$

where the satellite dependent bias has canceled out. For moderate distances between the base and the rover site, the satellite-receiver specific biases are highly correlated. Therefore, the influence of radial orbital errors and

of refraction is significantly reduced. Neglecting these biases, Eq. (8.23) simplifies to

$$R_B^j(t)_{\text{corr}} = \varrho_B^j(t) + \Delta\varrho_{AB}(t) \tag{8.24}$$

where $\Delta\varrho_{AB}(t) = \Delta\varrho_B(t) - \Delta\varrho_A(t)$. If multipath is neglected, this term converts to the combined receiver clock bias scaled to range, i.e., $\Delta\varrho_{AB}(t) = c\,\delta_{AB}(t) = c\,\delta_B(t) - c\,\delta_A(t)$. If no latency exists, the equation above is identical with the between-receiver single-difference of code ranges measured at A and B, and differential positioning converts to relative positioning (Sect. 8.3).

Positioning at the rover site B is performed with the corrected code pseudoranges $R_B^j(t)_{\text{corr}}$ leading to improved positional accuracies. The basic configuration for DGPS with code ranges is identical with that for kinematic point positioning with code ranges, cf. Eq. (8.8).

8.2.3 DGPS with phase ranges

Generalizing (8.9) and following Lichtenegger (1998), the phase pseudorange measured at the base station A at epoch t_0 can be modeled by

$$\lambda\,\Phi_A^j(t_0) = \varrho_A^j(t_0) + \Delta\varrho_A^j(t_0) + \Delta\varrho^j(t_0) + \Delta\varrho_A(t_0) + \lambda\,N_A^j \tag{8.25}$$

where again, in analogy to the code range model, $\varrho_A^j(t_0)$ is the geometric range, $\Delta\varrho_A^j(t_0)$ is the satellite-receiver dependent bias, $\Delta\varrho^j(t_0)$ is purely satellite dependent, $\Delta\varrho_A(t_0)$ is purely receiver dependent. Finally, N_A^j is the phase ambiguity. Consequently, the phase range correction at reference epoch t_0 is given by

$$\begin{aligned} \text{PRC}^j(t_0) &= \varrho_A^j(t_0) - \lambda\,\Phi_A^j(t_0) \\ &= -\Delta\varrho_A^j(t_0) - \Delta\varrho^j(t_0) - \Delta\varrho_A(t_0) - \lambda\,N_A^j\,. \end{aligned} \tag{8.26}$$

The formulation of range rate corrections in the base station A as well as the application of predicted range corrections to the observed phase ranges in the rover site B is carried out in full analogy to the previously described code range procedure. Therefore,

$$\lambda\,\Phi_B^j(t)_{\text{corr}} = \varrho_B^j(t) + \Delta\varrho_{AB}(t) + \lambda\,N_{AB}^j \tag{8.27}$$

results for the corrected phase ranges where $\Delta\varrho_{AB}(t) = \Delta\varrho_B(t) - \Delta\varrho_A(t)$ and $N_{AB}^j = N_B^j - N_A^j$ is the (single-) difference of the phase ambiguities. As in the code range model, if multipath is neglected, the term $\Delta\varrho_{AB}(t)$ converts to the combined receiver clock bias scaled to range, i.e., $\Delta\varrho_{AB}(t) = c\,\delta_{AB}(t) = c\,\delta_B(t) - c\,\delta_A(t)$.

Point positioning at the rover site B is performed with the corrected phase pseudoranges $\lambda\,\Phi_B^j(t)_{\text{corr}}$. The basic configuration for DGPS with phase ranges is identical with that for kinematic point positioning with phase ranges, cf. Eq. (8.14).

DGPS with phase ranges, sometimes denoted as carrier phase differential technique, is used for most precise real-time kinematic applications. For this mode of operation, OTF techniques are required to resolve the ambiguities. Note that for these techniques at least five common satellites must be observed in the base and in the rover station. Note also that differential DGPS with phases converts to RTK if the latency becomes zero.

8.3 Relative positioning

The objective of relative positioning is to determine the coordinates of an unknown point with respect to a known point which, for most applications, is stationary. In other words, relative positioning aims at the determination of the vector between the two points which is often called the baseline vector or simply baseline (Fig. 7.2). Let A denote the (known) reference point, B the unknown point, and $\underline{b}_{AB}$ the baseline vector. Introducing the corresponding position vectors $\underline{X}_A$, $\underline{X}_B$, the relation

$$\underline{X}_B = \underline{X}_A + \underline{b}_{AB} \tag{8.28}$$

may be formulated, and the components of the baseline vector $\underline{b}_{AB}$ are

$$\underline{b}_{AB} = \begin{bmatrix} X_B - X_A \\ Y_B - Y_A \\ Z_B - Z_A \end{bmatrix} = \begin{bmatrix} \Delta X_{AB} \\ \Delta Y_{AB} \\ \Delta Z_{AB} \end{bmatrix}. \tag{8.29}$$

The coordinates of the reference point must be given in the WGS-84 system and are usually approximated by a code range solution.

Relative positioning can be performed with code ranges, cf. Eq. 8.5), or with phase ranges, cf. Eq. (8.10). Subsequently, only phase ranges are explicitly considered. Relative positioning requires simultaneous observations at both the reference and the unknown point. This means that the observation time tags for the two points must be the same. Assuming such simultaneous observations at the two points A and B to satellites j and k, linear combinations can be formed leading to single-differences, double-differences, and triple-differences. Differencing can basically be accomplished in three different ways: across receivers, across satellites, across time (Logsdon 1992: p. 96). Instead of "across" frequently "between" is used. In order to avoid overburdened expressions, shorthand notations

will be used throughout the textbook with the following meanings: single-difference corresponds to across-receiver difference (or between-receiver difference), double-difference corresponds to across-receiver and across-satellite difference, and triple-difference corresponds to across-receiver and across-satellite and across-time difference. Most postprocessing software uses these three difference techniques, so their basic mathematical modeling is shown in the following sections.

8.3.1 Phase differences

Single-differences
Two points and one satellite are involved. Denoting the points by A and B and the satellite by j and using Eq. (8.10), the phase equations for the two points are

$$\begin{aligned}\Phi_A^j(t) + f^j\,\delta^j(t) &= \frac{1}{\lambda}\,\varrho_A^j(t) + N_A^j + f^j\,\delta_A(t)\\ \Phi_B^j(t) + f^j\,\delta^j(t) &= \frac{1}{\lambda}\,\varrho_B^j(t) + N_B^j + f^j\,\delta_B(t)\end{aligned} \tag{8.30}$$

and the difference of the two equations is

$$\begin{aligned}\Phi_B^j(t) - \Phi_A^j(t) &= \frac{1}{\lambda}\left[\varrho_B^j(t) - \varrho_A^j(t)\right] + N_B^j - N_A^j\\ &\quad + f^j\left[\delta_B(t) - \delta_A(t)\right].\end{aligned} \tag{8.31}$$

Equation (8.31) is referred to as the single-difference equation. This equation stresses one aspect of the solution for the unknowns on the right side. A system of such equations would lead to a rank deficiency even in the case of an arbitrarily large redundancy. This means that the design matrix of the adjustment has linearly dependent columns and a rank deficiency exists. Therefore, the relative quantities

$$\begin{aligned}N_{AB}^j &= N_B^j - N_A^j\\ \delta_{AB}(t) &= \delta_B(t) - \delta_A(t)\end{aligned} \tag{8.32}$$

are introduced. Using additionally the shorthand notations

$$\begin{aligned}\Phi_{AB}^j(t) &= \Phi_B^j(t) - \Phi_A^j(t)\\ \varrho_{AB}^j(t) &= \varrho_B^j(t) - \varrho_A^j(t),\end{aligned} \tag{8.33}$$

and substituting (8.32) and (8.33) into (8.31) gives

$$\Phi_{AB}^j(t) = \frac{1}{\lambda}\,\varrho_{AB}^j(t) + N_{AB}^j + f^j\,\delta_{AB}(t) \tag{8.34}$$

which is the final form of the single-difference equation. Note that the satellite clock bias has canceled, compared to the phase equation (8.10).

Double-differences
Assuming the two points A, B, and the two satellites j, k, two single-differences according to Eq. (8.34) may be formed:

$$\begin{aligned}\Phi_{AB}^j(t) &= \frac{1}{\lambda}\,\varrho_{AB}^j(t) + N_{AB}^j + f^j\,\delta_{AB}(t)\\ \Phi_{AB}^k(t) &= \frac{1}{\lambda}\,\varrho_{AB}^k(t) + N_{AB}^k + f^k\,\delta_{AB}(t).\end{aligned} \tag{8.35}$$

To obtain a double-difference, these single-differences are subtracted. Assuming equal frequencies $f^j = f^k$ for the satellite signals, the result is

$$\Phi_{AB}^k(t) - \Phi_{AB}^j(t) = \frac{1}{\lambda}\left[\varrho_{AB}^k(t) - \varrho_{AB}^j(t)\right] + N_{AB}^k - N_{AB}^j. \tag{8.36}$$

Using shorthand notations for the satellites j and k analogously to (8.33), the final form of the double-difference equation is

$$\Phi_{AB}^{jk}(t) = \frac{1}{\lambda}\,\varrho_{AB}^{jk}(t) + N_{AB}^{jk}. \tag{8.37}$$

The canceling effect of the receiver clock biases is the reason why double-differences are preferably used. This cancellation resulted from the assumptions of simultaneous observations and equal frequencies of the satellite signals.

Symbolically, the convention

$$*_{AB}^{jk} = *_{AB}^{k} - *_{AB}^{j} \tag{8.38}$$

has been introduced where the asterisk may be replaced by Φ, ϱ, or N. Note that these terms comprising two subscripts and two superscripts are actually composed of four terms. The symbolic notation

$$*_{AB}^{jk} = *_{B}^{k} - *_{B}^{j} - *_{A}^{k} + *_{A}^{j} \tag{8.39}$$

characterizes, in detail, the terms in the double-difference equation:

$$\begin{aligned}\Phi_{AB}^{jk}(t) &= \Phi_B^k(t) - \Phi_B^j(t) - \Phi_A^k(t) + \Phi_A^j(t)\\ \varrho_{AB}^{jk}(t) &= \varrho_B^k(t) - \varrho_B^j(t) - \varrho_A^k(t) + \varrho_A^j(t)\\ N_{AB}^{jk} &= N_B^k - N_B^j - N_A^k + N_A^j.\end{aligned} \tag{8.40}$$

Triple-differences
So far only one epoch t has been considered. To eliminate the time independent ambiguities, Remondi (1984) has suggested differencing double-differences between two epochs. Denoting the two epochs by t_1 and t_2, then

$$\begin{aligned}\Phi_{AB}^{jk}(t_1) &= \frac{1}{\lambda}\varrho_{AB}^{jk}(t_1) + N_{AB}^{jk} \\ \Phi_{AB}^{jk}(t_2) &= \frac{1}{\lambda}\varrho_{AB}^{jk}(t_2) + N_{AB}^{jk}\end{aligned} \tag{8.41}$$

are the two double-differences, and

$$\Phi_{AB}^{jk}(t_2) - \Phi_{AB}^{jk}(t_1) = \frac{1}{\lambda}\left[\varrho_{AB}^{jk}(t_2) - \varrho_{AB}^{jk}(t_1)\right] \tag{8.42}$$

is the triple-difference which may be written in the simplified form

$$\Phi_{AB}^{jk}(t_{12}) = \frac{1}{\lambda}\varrho_{AB}^{jk}(t_{12}) \tag{8.43}$$

if the symbolic formula

$$*(t_{12}) = *(t_2) - *(t_1) \tag{8.44}$$

is applied to the terms Φ and ϱ. It should be noted that both $\Phi_{AB}^{jk}(t_{12})$ and $\varrho_{AB}^{jk}(t_{12})$ are actually composed of eight terms each. Resubstituting (8.42) and either (8.39) or (8.40) yields

$$\begin{aligned}\Phi_{AB}^{jk}(t_{12}) \;=\; &+\Phi_B^k(t_2) - \Phi_B^j(t_2) - \Phi_A^k(t_2) + \Phi_A^j(t_2) \\ &-\Phi_B^k(t_1) + \Phi_B^j(t_1) + \Phi_A^k(t_1) - \Phi_A^j(t_1)\end{aligned} \tag{8.45}$$

and

$$\begin{aligned}\varrho_{AB}^{jk}(t_{12}) \;=\; &+\varrho_B^k(t_2) - \varrho_B^j(t_2) - \varrho_A^k(t_2) + \varrho_A^j(t_2) \\ &-\varrho_B^k(t_1) + \varrho_B^j(t_1) + \varrho_A^k(t_1) - \varrho_A^j(t_1)\,.\end{aligned} \tag{8.46}$$

The advantage of triple-differences is the canceling effect for the ambiguities and, thus, the immunity from changes in the ambiguities. Such changes are called cycle slips and are treated in more detail in Sect. 9.1.2.

8.3.2 Correlations of the phase combinations

In general, there are two groups of correlations, (1) the physical and (2) the mathematical correlations. The phases from one satellite received at two points, for example $\Phi_A^j(t)$ and $\Phi_B^j(t)$, are physically correlated since they refer to the same satellite. Usually, the physical correlation is not

taken into account. Therefore, main interest is directed to the mathematical correlations introduced by differencing.

The assumption may be made that the phase errors show a random behavior resulting in a normal distribution with expectation value zero and variance σ^2. Measured (or raw) phases are, therefore, linearly independent or uncorrelated. Introducing a vector $\underline{\Phi}$ containing the phases, then

$$\mathrm{cov}(\underline{\Phi}) = \sigma^2\,\underline{I} \tag{8.47}$$

is the covariance matrix for the phases where $\underline{I}$ is the unit matrix.

Single-differences
Considering the two points A, B and the satellite j at epoch t gives

$$\Phi_{AB}^j(t) = \Phi_B^j(t) - \Phi_A^j(t) \tag{8.48}$$

as the corresponding single-difference. Forming a second single-difference for the same two points but with another satellite k at the same epoch yields

$$\Phi_{AB}^k(t) = \Phi_B^k(t) - \Phi_A^k(t)\,. \tag{8.49}$$

The two single-differences may be computed from the matrix vector relation

$$\underline{SD} = \underline{C}\,\underline{\Phi} \tag{8.50}$$

where

$$\underline{SD} = \begin{bmatrix}\Phi_{AB}^j(t)\\ \Phi_{AB}^k(t)\end{bmatrix}$$

$$\underline{C} = \begin{bmatrix}-1 & 1 & 0 & 0\\ 0 & 0 & -1 & 1\end{bmatrix} \qquad \underline{\Phi} = \begin{bmatrix}\Phi_A^j(t)\\ \Phi_B^j(t)\\ \Phi_A^k(t)\\ \Phi_B^k(t)\end{bmatrix}. \tag{8.51}$$

The covariance law applied to Eq. (8.50) gives

$$\mathrm{cov}(\underline{SD}) = \underline{C}\,\mathrm{cov}(\underline{\Phi})\,\underline{C}^T \tag{8.52}$$

and, by substituting Eq. (8.47),

$$\mathrm{cov}(\underline{SD}) = \underline{C}\,\sigma^2\,\underline{I}\,\underline{C}^T = \sigma^2\,\underline{C}\,\underline{C}^T \tag{8.53}$$

is obtained. Taking $\underline{C}$ from (8.51), the matrix product

$$\underline{C}\,\underline{C}^T = 2\begin{bmatrix}1 & 0\\ 0 & 1\end{bmatrix} = 2\,\underline{I} \tag{8.54}$$

Using the notations $\underline{x}(t)$ for the predicted state vector, $\hat{\underline{x}}(t)$ for the updated state vector, and $\overset{\circ}{\underline{x}}(t)$ for the smoothed state vector, then a formula for optimal smoothing is

$$\overset{\circ}{\underline{x}}(t_i) = \hat{\underline{x}}(t_i) + \underline{D}(t_{i+1}, t_i)\left[\overset{\circ}{\underline{x}}(t_{i+1}) - \underline{x}(t_{i+1})\right] \tag{9.112}$$

where the gain matrix is

$$\underline{D}(t_{i+1}, t_i) = \underline{\hat{Q}}_{x_i}\, \underline{T}(t_{i+1}, t_i)\, \underline{Q}^{-1}_{x_{i+1}} \tag{9.113}$$

At the epoch of the last update measurement, the updated state vector is set identical to the smoothed one, and the backwards algorithm can be started. From Eq. (9.112), one may conclude that the process requires the predicted and updated vectors and the cofactor matrices at the update epochs as well as the transition matrices between the updates. This implies, in general, a large amount of data. This is probably the reason why optimal smoothing is very often replaced by empirical methods.

9.4 Adjustment of mathematical GPS models

9.4.1 Linearization

When the models of Chap. 8 are considered, the only term comprising unknowns in nonlinear form is ϱ. This section explains in detail how ϱ is linearized. The basic formula from Eq. (8.2)

$$\begin{aligned}\varrho_i^j(t) &= \sqrt{(X^j(t) - X_i)^2 + (Y^j(t) - Y_i)^2 + (Z^j(t) - Z_i)^2} \\ &\equiv f(X_i, Y_i, Z_i)\end{aligned} \tag{9.114}$$

shows the unknown point coordinates X_i, Y_i, Z_i in nonlinear form. Assuming approximate values X_{i0}, Y_{i0}, Z_{i0} for the unknowns, an approximate distance $\varrho_{i0}^j(t)$ can be calculated by

$$\begin{aligned}\varrho_{i0}^j(t) &= \sqrt{(X^j(t) - X_{i0})^2 + (Y^j(t) - Y_{i0})^2 + (Z^j(t) - Z_{i0})^2} \\ &\equiv f(X_{i0}, Y_{i0}, Z_{i0})\,.\end{aligned} \tag{9.115}$$

Using approximate values, the unknowns X_i, Y_i, Z_i can be decomposed by

$$\begin{aligned}X_i &= X_{i0} + \Delta X_i \\ Y_i &= Y_{i0} + \Delta Y_i \\ Z_i &= Z_{i0} + \Delta Z_i\end{aligned} \tag{9.116}$$

where now ΔX_i, ΔY_i, ΔZ_i are new unknowns. This means that the original unknowns have been split into a known part (represented by the approximate values X_{i0}, Y_{i0}, Z_{i0}) and an unknown part (represented by ΔX_i, ΔY_i, ΔZ_i). The advantage of this splitting-up is that the function $f(X_i, Y_i, Z_i)$ is replaced by an equivalent function $f(X_{i0} + \Delta X_i, Y_{i0} + \Delta Y_i, Z_{i0} + \Delta Z_i)$ which can now be expanded into a Taylor series with respect to the approximate point. This leads to

$$\begin{aligned}f(X_i, Y_i, Z_i) &\equiv f(X_{i0} + \Delta X_i, Y_{i0} + \Delta Y_i, Z_{i0} + \Delta Z_i) \\ &= f(X_{i0}, Y_{i0}, Z_{i0}) + \frac{\partial f(X_{i0}, Y_{i0}, Z_{i0})}{\partial X_{i0}}\Delta X_i \\ &+ \frac{\partial f(X_{i0}, Y_{i0}, Z_{i0})}{\partial Y_{i0}}\Delta Y_i + \frac{\partial f(X_{i0}, Y_{i0}, Z_{i0})}{\partial Z_{i0}}\Delta Z_i + \ldots\end{aligned} \tag{9.117}$$

where the expansion is truncated after the linear term; otherwise, the unknowns ΔX_i, ΔY_i, ΔZ_i would appear in nonlinear form. The partial derivatives are obtained from (9.115) by

$$\begin{aligned}\frac{\partial f(X_{i0}, Y_{i0}, Z_{i0})}{\partial X_{i0}} &= -\frac{X^j(t) - X_{i0}}{\varrho_{i0}^j(t)} \\ \frac{\partial f(X_{i0}, Y_{i0}, Z_{i0})}{\partial Y_{i0}} &= -\frac{Y^j(t) - Y_{i0}}{\varrho_{i0}^j(t)} \\ \frac{\partial f(X_{i0}, Y_{i0}, Z_{i0})}{\partial Z_{i0}} &= -\frac{Z^j(t) - Z_{i0}}{\varrho_{i0}^j(t)}\end{aligned} \tag{9.118}$$

and are the components of the unit vector pointing from the satellite towards the approximate site. The substitution of Eqs. (9.115) and (9.118) into Eq. (9.117) gives

$$\begin{aligned}\varrho_i^j(t) = \varrho_{i0}^j(t) &- \frac{X^j(t) - X_{i0}}{\varrho_{i0}^j(t)}\Delta X_i - \frac{Y^j(t) - Y_{i0}}{\varrho_{i0}^j(t)}\Delta Y_i \\ &- \frac{Z^j(t) - Z_{i0}}{\varrho_{i0}^j(t)}\Delta Z_i\end{aligned} \tag{9.119}$$

where the equivalence of $f(X_i, Y_i, Z_i)$ with $\varrho_i^j(t)$ has been used. This equation is now linear with respect to the unknowns ΔX_i, ΔY_i, ΔZ_i.

9.4.2 Linear model for point positioning with code ranges

The model is given only in its elementary form and, thus, apart from the geometry, only the clocks are modeled. The ionosphere, troposphere, and

other minor effects are neglected. According to Eq. (8.5), the model for point positioning with code ranges is given by

$$R_i^j(t) = \varrho_i^j(t) + c\,\delta_i(t) - c\,\delta^j(t) \tag{9.120}$$

which can be linearized by substituting (9.119):

$$\begin{aligned} R_i^j(t) = \varrho_{i0}^j(t) - \frac{X^j(t) - X_{i0}}{\varrho_{i0}^j(t)}\,\Delta X_i + \frac{Y^j(t) - Y_{i0}}{\varrho_{i0}^j(t)}\,\Delta Y_i \\ - \frac{Z^j(t) - Z_{i0}}{\varrho_{i0}^j(t)}\,\Delta Z_i + c\,\delta_i(t) - c\,\delta^j(t)\,. \end{aligned} \tag{9.121}$$

Leaving the terms containing unknowns on the right side, the equation above is rewritten as

$$\begin{aligned} R_i^j(t) - \varrho_{i0}^j(t) + c\,\delta^j(t) = -\frac{X^j(t) - X_{i0}}{\varrho_{i0}^j(t)}\,\Delta X_i \\ - \frac{Y^j(t) - Y_{i0}}{\varrho_{i0}^j(t)}\,\Delta Y_i - \frac{Z^j(t) - Z_{i0}}{\varrho_{i0}^j(t)}\,\Delta Z_i + c\,\delta_i(t) \end{aligned} \tag{9.122}$$

where the satellite clock bias is assumed to be known. This assumption makes sense because satellite clock correctors can be received from the navigation message. Model (9.122) comprises (for the epoch t) four unknowns, namely ΔX_i, ΔY_i, ΔZ_i, $\delta_i(t)$. Consequently, four satellites are needed to solve the problem. The shorthand notations

$$\begin{aligned} \ell^j &= R_i^j(t) - \varrho_{i0}^j(t) + c\,\delta^j(t) \\ a_{X_i}^j &= -\frac{X^j(t) - X_{i0}}{\varrho_{i0}^j(t)} \\ a_{Y_i}^j &= -\frac{Y^j(t) - Y_{i0}}{\varrho_{i0}^j(t)} \\ a_{Z_i}^j &= -\frac{Z^j(t) - Z_{i0}}{\varrho_{i0}^j(t)} \end{aligned} \tag{9.123}$$

help to simplify the representation of the system of equations. Assuming now four satellites numbered from 1 to 4, then

$$\begin{aligned} \ell^1 &= a_{X_i}^1\,\Delta X_i + a_{Y_i}^1\,\Delta Y_i + a_{Z_i}^1\,\Delta Z_i + c\,\delta_i(t) \\ \ell^2 &= a_{X_i}^2\,\Delta X_i + a_{Y_i}^2\,\Delta Y_i + a_{Z_i}^2\,\Delta Z_i + c\,\delta_i(t) \\ \ell^3 &= a_{X_i}^3\,\Delta X_i + a_{Y_i}^3\,\Delta Y_i + a_{Z_i}^3\,\Delta Z_i + c\,\delta_i(t) \\ \ell^4 &= a_{X_i}^4\,\Delta X_i + a_{Y_i}^4\,\Delta Y_i + a_{Z_i}^4\,\Delta Z_i + c\,\delta_i(t) \end{aligned} \tag{9.124}$$

is the appropriate system of equations. Note that the superscripts are the satellite numbers and not exponents! Introducing

$$\underline{A} = \begin{bmatrix} a_{X_i}^1 & a_{Y_i}^1 & a_{Z_i}^1 & c \\ a_{X_i}^2 & a_{Y_i}^2 & a_{Z_i}^2 & c \\ a_{X_i}^3 & a_{Y_i}^3 & a_{Z_i}^3 & c \\ a_{X_i}^4 & a_{Y_i}^4 & a_{Z_i}^4 & c \end{bmatrix} \quad \underline{x} = \begin{bmatrix} \Delta X_i \\ \Delta Y_i \\ \Delta Z_i \\ \delta_i(t) \end{bmatrix} \quad \underline{\ell} = \begin{bmatrix} \ell^1 \\ \ell^2 \\ \ell^3 \\ \ell^4 \end{bmatrix}, \tag{9.125}$$

the set of linear equations can be written in the matrix–vector form

$$\underline{\ell} = \underline{A}\,\underline{x}\,. \tag{9.126}$$

For this first example of a linearized GPS model, the resubstitution of the vector $\underline{\ell}$ and the matrix $\underline{A}$ using (9.123) is given explicitly for one epoch t:

$$\underline{\ell} = \begin{bmatrix} R_i^1(t) - \varrho_{i0}^1(t) + c\,\delta^1(t) \\ R_i^2(t) - \varrho_{i0}^2(t) + c\,\delta^2(t) \\ R_i^3(t) - \varrho_{i0}^3(t) + c\,\delta^3(t) \\ R_i^4(t) - \varrho_{i0}^4(t) + c\,\delta^4(t) \end{bmatrix}$$

$$\underline{A} = \begin{bmatrix} -\dfrac{X^1(t) - X_{i0}}{\varrho_{i0}^1(t)} & -\dfrac{Y^1(t) - Y_{i0}}{\varrho_{i0}^1(t)} & -\dfrac{Z^1(t) - Z_{i0}}{\varrho_{i0}^1(t)} & c \\ -\dfrac{X^2(t) - X_{i0}}{\varrho_{i0}^2(t)} & -\dfrac{Y^2(t) - Y_{i0}}{\varrho_{i0}^2(t)} & -\dfrac{Z^2(t) - Z_{i0}}{\varrho_{i0}^2(t)} & c \\ -\dfrac{X^3(t) - X_{i0}}{\varrho_{i0}^3(t)} & -\dfrac{Y^3(t) - Y_{i0}}{\varrho_{i0}^3(t)} & -\dfrac{Z^3(t) - Z_{i0}}{\varrho_{i0}^3(t)} & c \\ -\dfrac{X^4(t) - X_{i0}}{\varrho_{i0}^4(t)} & -\dfrac{Y^4(t) - Y_{i0}}{\varrho_{i0}^4(t)} & -\dfrac{Z^4(t) - Z_{i0}}{\varrho_{i0}^4(t)} & c \end{bmatrix}. \tag{9.127}$$

From the linear system (9.126), the coordinate differences ΔX_i, ΔY_i, ΔZ_i and the receiver clock error $\delta_i(t)$ for epoch t result. The desired point coordinates are finally obtained by (9.116).

Recall that the selection of the approximate values for the coordinates was completely arbitrary; they could even be set equal to zero (but this might require an iteration).

Point positioning with code ranges is applicable for each epoch separately. Therefore, this model may also be used in kinematic applications.

where the different time epochs have been inserted accordingly. The solution of this redundant system is performed by least squares adjustment.

9.4.4 Linear model for relative positioning

The previous sections have shown linear models for both code ranges and carrier phases. For the case of relative positioning, the investigation is restricted to carrier phases, since it should be obvious how to change from the more expanded model of phases to a code model. Furthermore, the linearization and setup of the linear equation system remains, in principle, the same for phases and phase combinations and could be performed analogously for each model. Therefore, the double-difference is selected for treatment in detail. The model for the double-difference of Eq. (8.37), multiplied by λ, is

$$\lambda \Phi_{AB}^{jk}(t) = \varrho_{AB}^{jk}(t) + \lambda N_{AB}^{jk} \tag{9.131}$$

where the term ϱ_{AB}^{jk}, containing the geometry, is composed as

$$\varrho_{AB}^{jk}(t) = \varrho_B^k(t) - \varrho_B^j(t) - \varrho_A^k(t) + \varrho_A^j(t) \tag{9.132}$$

which reflects the fact of four measurement quantities for a double-difference. Each of the four terms must be linearized according to (9.119) yielding

$$\begin{aligned}
\varrho_{AB}^{jk}(t) = \; & \varrho_{B0}^k(t) - \frac{X^k(t) - X_{B0}}{\varrho_{B0}^k(t)} \Delta X_B - \frac{Y^k(t) - Y_{B0}}{\varrho_{B0}^k(t)} \Delta Y_B \\
& - \frac{Z^k(t) - Z_{B0}}{\varrho_{B0}^k(t)} \Delta Z_B \\
& - \varrho_{B0}^j(t) + \frac{X^j(t) - X_{B0}}{\varrho_{B0}^j(t)} \Delta X_B + \frac{Y^j(t) - Y_{B0}}{\varrho_{B0}^j(t)} \Delta Y_B \\
& + \frac{Z^j(t) - Z_{B0}}{\varrho_{B0}^j(t)} \Delta Z_B \\
& - \varrho_{A0}^k(t) + \frac{X^k(t) - X_{A0}}{\varrho_{A0}^k(t)} \Delta X_A + \frac{Y^k(t) - Y_{A0}}{\varrho_{A0}^k(t)} \Delta Y_A \\
& + \frac{Z^k(t) - Z_{A0}}{\varrho_{A0}^k(t)} \Delta Z_A \\
& + \varrho_{A0}^j(t) - \frac{X^j(t) - X_{A0}}{\varrho_{A0}^j(t)} \Delta X_A - \frac{Y^j(t) - Y_{A0}}{\varrho_{A0}^j(t)} \Delta Y_A \\
& - \frac{Z^j(t) - Z_{A0}}{\varrho_{A0}^j(t)} \Delta Z_A \,.
\end{aligned} \tag{9.133}$$

Substituting (9.133) into (9.131) and rearranging leads to the linear observation equation

$$\begin{aligned}
\ell_{AB}^{jk}(t) = \; & a_{X_A}^{jk}(t)\,\Delta X_A + a_{Y_A}^{jk}(t)\,\Delta Y_A + a_{Z_A}^{jk}(t)\,\Delta Z_A \\
& + a_{X_B}^{jk}(t)\,\Delta X_B + a_{Y_B}^{jk}(t)\,\Delta Y_B + a_{Z_B}^{jk}(t)\,\Delta Z_B + \lambda N_{AB}^{jk}
\end{aligned} \tag{9.134}$$

where the left side

$$\ell_{AB}^{jk}(t) = \lambda \Phi_{AB}^{jk}(t) - \varrho_{B0}^k(t) + \varrho_{B0}^j(t) + \varrho_{A0}^k(t) - \varrho_{A0}^j(t) \tag{9.135}$$

comprises both the measurement quantities and all terms computed from the approximate values. On the right side of (9.134), the abbreviations

$$\begin{aligned}
a_{X_A}^{jk}(t) &= +\frac{X^k(t) - X_{A0}}{\varrho_{A0}^k(t)} - \frac{X^j(t) - X_{A0}}{\varrho_{A0}^j(t)} \\
a_{Y_A}^{jk}(t) &= +\frac{Y^k(t) - Y_{A0}}{\varrho_{A0}^k(t)} - \frac{Y^j(t) - Y_{A0}}{\varrho_{A0}^j(t)} \\
a_{Z_A}^{jk}(t) &= +\frac{Z^k(t) - Z_{A0}}{\varrho_{A0}^k(t)} - \frac{Z^j(t) - Z_{A0}}{\varrho_{A0}^j(t)} \\
a_{X_B}^{jk}(t) &= -\frac{X^k(t) - X_{B0}}{\varrho_{B0}^k(t)} + \frac{X^j(t) - X_{B0}}{\varrho_{B0}^j(t)} \\
a_{Y_B}^{jk}(t) &= -\frac{Y^k(t) - Y_{B0}}{\varrho_{B0}^k(t)} + \frac{Y^j(t) - Y_{B0}}{\varrho_{B0}^j(t)} \\
a_{Z_B}^{jk}(t) &= -\frac{Z^k(t) - Z_{B0}}{\varrho_{B0}^k(t)} + \frac{Z^j(t) - Z_{B0}}{\varrho_{B0}^j(t)}
\end{aligned} \tag{9.136}$$

have been used. Note that the coordinates of one point (e.g., A) must be known for relative positioning. More specifically, the known point A reduces the number of unknowns by three because of

$$\Delta X_A = \Delta Y_A = \Delta Z_A = 0 \tag{9.137}$$

and leads to a slight change in the left side term

$$\ell_{AB}^{jk}(t) = \lambda \Phi_{AB}^{jk}(t) - \varrho_{B0}^k(t) + \varrho_{B0}^j(t) + \varrho_A^k(t) - \varrho_A^j(t)\,. \tag{9.138}$$

9.4.3 Linear model for point positioning with carrier phases

The procedure is the same as in the previous section. In Eq. (8.10), the linearization is performed for $\varrho_i^j(t)$, and known terms are shifted to the left side. Multiplying the equation by λ and using $c = \lambda f$, the result is

$$\begin{aligned}\lambda\,\Phi_i^j(t) - \varrho_{i0}^j(t) + c\,\delta^j(t) = &-\frac{X^j(t) - X_{i0}}{\varrho_{i0}^j(t)}\,\Delta X_i \\ -\frac{Y^j(t) - Y_{i0}}{\varrho_{i0}^j(t)}\,\Delta Y_i &- \frac{Z^j(t) - Z_{i0}}{\varrho_{i0}^j(t)}\,\Delta Z_i + \lambda\,N_i^j + c\,\delta_i(t)\end{aligned} \tag{9.128}$$

where, compared to point positioning with code ranges, the number of unknowns is now increased by the ambiguities. Considering again four satellites, the system is given in matrix–vector form $\underline{\ell} = \underline{A}\,\underline{x}$ where

$$\underline{\ell} = \begin{bmatrix} \lambda\,\Phi_i^1(t) - \varrho_{i0}^1(t) + c\,\delta^1(t) \\ \lambda\,\Phi_i^2(t) - \varrho_{i0}^2(t) + c\,\delta^2(t) \\ \lambda\,\Phi_i^3(t) - \varrho_{i0}^3(t) + c\,\delta^3(t) \\ \lambda\,\Phi_i^4(t) - \varrho_{i0}^4(t) + c\,\delta^4(t) \end{bmatrix}$$

$$\underline{A} = \begin{bmatrix} a_{X_i}^1(t) & a_{Y_i}^1(t) & a_{Z_i}^1(t) & \lambda & 0 & 0 & 0 & c \\ a_{X_i}^2(t) & a_{Y_i}^2(t) & a_{Z_i}^2(t) & 0 & \lambda & 0 & 0 & c \\ a_{X_i}^3(t) & a_{Y_i}^3(t) & a_{Z_i}^3(t) & 0 & 0 & \lambda & 0 & c \\ a_{X_i}^4(t) & a_{Y_i}^4(t) & a_{Z_i}^4(t) & 0 & 0 & 0 & \lambda & c \end{bmatrix} \tag{9.129}$$

$$\underline{x}^T = \begin{bmatrix} \Delta X_i & \Delta Y_i & \Delta Z_i & N_i^1 & N_i^2 & N_i^3 & N_i^4 & \delta_i(t) \end{bmatrix}$$

and where the coefficients of the coordinate increments, cf. (9.123), are supplemented with the time parameter t. Obviously, the four equations do not solve for the eight unknowns. This reflects the fact that point positioning with phases in this form cannot be solved epoch by epoch. Each additional epoch increases the number of unknowns by a new clock term. Thus, for two epochs there are eight equations and nine unknowns (still an underdetermined problem). For three epochs there are 12 equations and 10 unknowns, thus, a slightly overdetermined problem. The 10 unknowns in the latter example are the coordinate increments ΔX_i, ΔY_i, ΔZ_i for the unknown point, the integer ambiguities N_i^1, N_i^2, N_i^3, N_i^4 for the four satellites, and the receiver clock biases $\delta_i(t_1)$, $\delta_i(t_2)$, $\delta_i(t_3)$ for the three epochs.

The matrix–vector scheme for the last example is given by

$$\underline{\ell} = \begin{bmatrix} \lambda\,\Phi_i^1(t_1) - \varrho_{i0}^1(t_1) + c\,\delta^1(t_1) \\ \lambda\,\Phi_i^2(t_1) - \varrho_{i0}^2(t_1) + c\,\delta^2(t_1) \\ \lambda\,\Phi_i^3(t_1) - \varrho_{i0}^3(t_1) + c\,\delta^3(t_1) \\ \lambda\,\Phi_i^4(t_1) - \varrho_{i0}^4(t_1) + c\,\delta^4(t_1) \\ \lambda\,\Phi_i^1(t_2) - \varrho_{i0}^1(t_2) + c\,\delta^1(t_2) \\ \lambda\,\Phi_i^2(t_2) - \varrho_{i0}^2(t_2) + c\,\delta^2(t_2) \\ \lambda\,\Phi_i^3(t_2) - \varrho_{i0}^3(t_2) + c\,\delta^3(t_2) \\ \lambda\,\Phi_i^4(t_2) - \varrho_{i0}^4(t_2) + c\,\delta^4(t_2) \\ \lambda\,\Phi_i^1(t_3) - \varrho_{i0}^1(t_3) + c\,\delta^1(t_3) \\ \lambda\,\Phi_i^2(t_3) - \varrho_{i0}^2(t_3) + c\,\delta^2(t_3) \\ \lambda\,\Phi_i^3(t_3) - \varrho_{i0}^3(t_3) + c\,\delta^3(t_3) \\ \lambda\,\Phi_i^4(t_3) - \varrho_{i0}^4(t_3) + c\,\delta^4(t_3) \end{bmatrix} \qquad \underline{x} = \begin{bmatrix} \Delta X_i \\ \Delta Y_i \\ \Delta Z_i \\ N_i^1 \\ N_i^2 \\ N_i^3 \\ N_i^4 \\ \delta_i(t_1) \\ \delta_i(t_2) \\ \delta_i(t_3) \end{bmatrix}$$

$$\underline{A} = \begin{bmatrix} a_{X_i}^1(t_1) & a_{Y_i}^1(t_1) & a_{Z_i}^1(t_1) & \lambda & 0 & 0 & 0 & c & 0 & 0 \\ a_{X_i}^2(t_1) & a_{Y_i}^2(t_1) & a_{Z_i}^2(t_1) & 0 & \lambda & 0 & 0 & c & 0 & 0 \\ a_{X_i}^3(t_1) & a_{Y_i}^3(t_1) & a_{Z_i}^3(t_1) & 0 & 0 & \lambda & 0 & c & 0 & 0 \\ a_{X_i}^4(t_1) & a_{Y_i}^4(t_1) & a_{Z_i}^4(t_1) & 0 & 0 & 0 & \lambda & c & 0 & 0 \\ a_{X_i}^1(t_2) & a_{Y_i}^1(t_2) & a_{Z_i}^1(t_2) & \lambda & 0 & 0 & 0 & 0 & c & 0 \\ a_{X_i}^2(t_2) & a_{Y_i}^2(t_2) & a_{Z_i}^2(t_2) & 0 & \lambda & 0 & 0 & 0 & c & 0 \\ a_{X_i}^3(t_2) & a_{Y_i}^3(t_2) & a_{Z_i}^3(t_2) & 0 & 0 & \lambda & 0 & 0 & c & 0 \\ a_{X_i}^4(t_2) & a_{Y_i}^4(t_2) & a_{Z_i}^4(t_2) & 0 & 0 & 0 & \lambda & 0 & c & 0 \\ a_{X_i}^1(t_3) & a_{Y_i}^1(t_3) & a_{Z_i}^1(t_3) & \lambda & 0 & 0 & 0 & 0 & 0 & c \\ a_{X_i}^2(t_3) & a_{Y_i}^2(t_3) & a_{Z_i}^2(t_3) & 0 & \lambda & 0 & 0 & 0 & 0 & c \\ a_{X_i}^3(t_3) & a_{Y_i}^3(t_3) & a_{Z_i}^3(t_3) & 0 & 0 & \lambda & 0 & 0 & 0 & c \\ a_{X_i}^4(t_3) & a_{Y_i}^4(t_3) & a_{Z_i}^4(t_3) & 0 & 0 & 0 & \lambda & 0 & 0 & c \end{bmatrix} \tag{9.130}$$

Abbreviations

AFB	Air Force Base
AOC	Auxiliary Output Chip
AROF	Ambiguity Resolution On-the-Fly
A-S	Anti-Spoofing
AVL	Automatic Vehicle Location
C/A	Coarse/Acquisition
CBIS	Central Bureau Information System
CDMA	Code Division Multiple Access
CEP	Celestial Ephemeris Pole
CEP	Circular Error Probable
CGSIC	Civil GPS Service Interface Committee
CHAMP	Challenging Mini-satellite Payload
CIGNET	Cooperative International GPS Network
CIO	Conventional International Origin
CODE	Center for Orbit Determination in Europe
CORS	Continuously Operating Reference Station
CRF	Celestial Reference Frame
CSOC	Consolidated Space Operations Center
DARC	Data Radio Channel
DGPS	Differential GPS
DLL	Delay Lock Loop
DMA	Defense Mapping Agency
DME	Distance Measuring Equipment
DoD	Department of Defense
DOP	Dilution of Precision
DOSE	Dynamics of Solid Earth
DoT	Department of Transportation
DRMS	Distance Root Mean Square (error)
ECEF	Earth-Centered-Earth-Fixed
EGM	Earth Gravitational Model
EGNOS	European Geostationary Navigation Overlay Service
EOP	Earth Orientation Parameters
ERS	Earth Remote Sensing (satellite)
FAA	Federal Aviation Administration
FDMA	Frequency Division Multiple Access
FGCC	Federal Geodetic Control Committee
FOC	Full Operational Capability

FRP	Federal Radionavigation Plan
FTP	File Transfer Protocol
GBAS	Ground-Based Augmentation System
GDOP	Geometric Dilution of Precision
GEO	Geostationary Orbit (satellite)
GIC	GPS Integrity Channel
GIM	Global Ionosphere Map
GIS	Geographic Information System
GLONASS	Global Navigation Satellite System
GNSS	Global Navigation Satellite System
GOTEX	Global Orbit Tracking Experiment
GPS	Global Positioning System
GRS	Geodetic Reference System
HDOP	Horizontal Dilution of Precision
HIRAN	High Range Navigation (system)
HOW	Hand-Over Word
IAG	International Association of Geodesy
IAT	International Atomic Time
IAU	International Astronomical Union
ICRF	IERS (or International) Celestial Reference Frame
IERS	International Earth Rotation Service
IF	Intermediate Frequency
IGEB	Interagency GPS Executive Board
IGEX	International GLONASS Experiment
IGS	International GPS Service (for Geodynamics)
ILS	Instrument Landing System
INMARSAT	International Maritime Satellite (organization)
INS	Inertial Navigation System
IOC	Initial Operational Capability
ION	Institute of Navigation
IRM	IERS (or International) Reference Meridian
IRP	IERS (or International) Reference Pole
ISU	International System of Units
ITRF	IERS (or International) Terrestrial Reference Frame
ITS	Intelligent Transportation System
ITU	International Telecommunication Union
IUGG	International Union for Geodesy and Geophysics
IVHS	Intelligent Vehicle/Highway System
IWV	Integrated Water Vapor
JD	Julian Date
JPL	Jet Propulsion Laboratory

JPO	Joint Program Office
LAAS	Local Area Augmentation System
LEO	Low Earth Orbit (satellite)
LEP	Linear Error Probable
LORAN	Long-Range Navigation (system)
MEDLL	Multipath Estimating Delay Lock Loop
MEO	Mean Earth Orbit (satellite)
MIT	Massachusetts Institute of Technology
MITES	Miniature Interferometer Terminals for Earth Surveying
MJD	Modified Julian Date
MLS	Microwave Landing System
MRSE	Mean Radial Spherical Error
NAD	North American Datum
NAGU	Notice Advisories to GLONASS Users
NANU	Notice Advisories to Navstar Users
NASA	National Aeronautics and Space Administration
NAVSTAR	Navigation System with Timing and Ranging
NGS	National Geodetic Survey
NIMA	National Imagery and Mapping Agency
NIS	Navigation Information Service
NMEA	National Marine Electronics Association
NNSS	Navy Navigation Satellite System (or TRANSIT)
NSWC	Naval Surface Warfare Center
OCS	Operational Control System
OEM	Original Equipment Manufacturer
OTF	On-the-Fly
OTR	On-the-Run
PCMCIA	PC Memory Card International Association
PDD	Presidential Decision Directive
PDOP	Position Dilution of Precision
PLL	Phase Lock Loop
PPS	Precise Positioning Service
PRC	Pseudorange Correction
PRN	Pseudorandom Noise
RAIM	Receiver Autonomous Integrity Monitoring
RDS	Radio Data System
RF	Radio Frequency
RINEX	Receiver Independent Exchange (format)
RRC	Range Rate Correction
RTCM	Radio Technical Commission for Maritime (services)
RTK	Real-Time Kinematic

SA	Selective Availability
SBAS	Satellite-Based Augmentation System
SD	Selective Denial
SEP	Spherical Error Probable
SERIES	Satellite Emission Range Inferred Earth Surveying
SINEX	Software Independent Exchange (format)
SLR	Satellite Laser Ranging
SNR	Signal-to-Noise Ratio
SPOT	Satellite Probatoire d'Observation de la Terre
SPS	Standard Positioning Service
SV	Space Vehicle
TACAN	Tactical Air Navigation
TCAR	Three-Carrier Ambiguity Resolution
TDOP	Time Dilution of Precision
TEC	Total Electron Content
TLM	Telemetry (word)
TOPEX	(Ocean) Topography Experiment
TOW	Time-of-Week (count)
TRF	Terrestrial Reference Frame
TT	Terrestrial Time
TVEC	Total Vertical Electron Content
UERE	User Equivalent Range Error
UHF	Ultra High Frequency
URL	Uniform Resource Locator
USCG	U.S. Coast Guard
USGS	U.S. Geological Survey
USNO	U.S. Naval Observatory
UT	Universal Time
UTC	Universal Time Coordinated
UTM	Universal Transverse Mercator (projection)
VDOP	Vertical Dilution of Precision
VHF	Very High Frequency
VLBI	Very Long Baseline Interferometry
VOR	VHF Omnidirectional Range (equipment)
VRS	Virtual Reference Station
WAAS	Wide Area Augmentation System
WADGPS	Wide Area Differential GPS
WGS	World Geodetic System
WRC	World Radio Conference
WWW	World Wide Web

Numerical constants

GPS signal frequencies		
$f_0 =$	10.23 MHz	fundamental frequency
L1 =	1 575.42 MHz	primary carrier frequency
L2 =	1 227.60 MHz	secondary carrier frequency

WGS-84		
a =	6 378 137.0 m	semimajor axis of ellipsoid
f =	$1/298.257\,223\,563$	flattening of ellipsoid
ω_E =	$7\,292\,115 \cdot 10^{-11}$ rad s^{-1}	angular velocity of the earth
GM =	$3\,986\,004.418 \cdot 10^{8}$ m^3 s^{-2}	earth's gravitational constant
b =	6 356 752.314 25 m	semiminor axis of ellipsoid
e^2 =	$6.694\,379\,990\,13 \cdot 10^{-3}$	first numerical eccentricity
e'^2 =	$6.739\,496\,742\,26 \cdot 10^{-3}$	second numerical eccentricity

Various constants		
c =	299 792 458 m s^{-1}	velocity of light
ω_E =	$7\,292\,115.1467 \cdot 10^{-11}$ rad s^{-1}	untruncated angular velocity
CD =	January 6.0, 1980	Civil date of GPS standard epoch
JD =	2 444 244.5	Julian date of GPS standard epoch